



# PROBING THE CARBON–PHOSPHORUS BOND COUPLING IN LOW-TEMPERATURE PHOSPHINE (PH<sub>3</sub>)–METHANE (CH<sub>4</sub>) INTERSTELLAR ICE ANALOGUES

ANDREW M. TURNER<sup>1,2</sup>, MATTHEW J. ABPLANALP<sup>1,2</sup>, AND RALF I. KAISER<sup>1,2</sup>

<sup>1</sup> W. M. Keck Research Laboratory in Astrochemistry, University of Hawaii at Manoa, Honolulu, HI 96822, USA

<sup>2</sup> Department of Chemistry, University of Hawaii at Manoa, Honolulu, HI 96822, USA

Received 2015 October 28; accepted 2016 February 2; published 2016 March 2

## ABSTRACT

Phosphine, which has now been confirmed around the carbon-rich star IRC+10216, provides the first example of a phosphorus-containing single bond in interstellar or circumstellar media. While four compounds containing both phosphorus and carbon have been discovered, none contain a carbon–phosphorus single bond. Here, we show that this moiety is plausible from the reaction of phosphine with methane in electron-irradiated interstellar ice analogues. Fractional sublimation allows for detection of individual products at distinct temperatures using reflectron time-of-flight mass spectrometry (ReTOF) coupled with vacuum ultraviolet photoionization. This method produced phosphanes and methylphosphanes as large as P<sub>8</sub>H<sub>10</sub> and CH<sub>3</sub>P<sub>8</sub>H<sub>9</sub>, which demonstrates that a phosphorus–carbon bond can readily form and that methylphosphanes sublime at 12–17 K higher temperatures than the non-organic phosphanes. Also, irradiated ices of phosphine with deuterated-methane untangle the reaction pathways through which these methylphosphanes were formed and identified radical recombination to be preferred over carbene/phosphinidene insertion reactions. In addition, these ReTOF results confirm that CH<sub>3</sub>PH<sub>2</sub> and CH<sub>6</sub>P<sub>2</sub> can form via insertion of carbene and phosphinidene and that the methylenediphosphine (PH<sub>2</sub>CH<sub>2</sub>PH<sub>2</sub>) isomer forms in the ices, although methylphosphine (CH<sub>3</sub>P<sub>2</sub>H<sub>3</sub>) is likely the more abundant isomer and that phosphanes and organophosphanes preferentially fragment via the loss of a phosphino group when photoionized. While the formation of methylphosphine is overall endoergic, the intermediates produced by interactions with energetic electrons proceed toward methylphosphine favorably and barrierlessly and provide plausible mechanisms toward hitherto unidentified interstellar compounds.

*Key words:* astrochemistry – ISM: molecules – methods: laboratory: solid state

## 1. INTRODUCTION

The recent discovery of phosphine (PH<sub>3</sub>) in the circumstellar envelope of the carbon-rich star IRC+10216 (CW Leonis) (Agúndez et al. 2008, 2014a; Tenenbaum & Ziurys 2008) at abundances of 10<sup>−8</sup> compared to molecular hydrogen (H<sub>2</sub>) has revitalized the interest in the interstellar phosphorus chemistry. Besides phosphine, only six phosphorus-bearing molecules have been discovered in interstellar and/or circumstellar environments (Figure 1). These are phosphorus nitride (PN) (Turner & Bally 1987; Ziurys 1987; Guélin et al. 2000; Milam et al. 2008), carbon phosphide (CP) (Guélin et al. 1990; Milam et al. 2008), phosphaethyne (HCP) (Agúndez et al. 2007; Milam et al. 2008), phosphorus monoxide (PO) (Tenenbaum et al. 2007), dicarbon phosphide (CCP) (Halfen et al. 2008), and cyanophosphaethyne (NCCP) (Agúndez et al. 2014b). Each of these, except for phosphorus monoxide (PO), has been detected along with phosphine (PH<sub>3</sub>) in IRC+10216 with abundances compared to molecular hydrogen of 3 × 10<sup>−10</sup> for phosphorus nitride (PN) (Milam et al. 2008), 5 × 10<sup>−9</sup> for carbon phosphide (CP) (Milam et al. 2008), 3 × 10<sup>−8</sup> for phosphaethyne (HCP) (Milam et al. 2008), 10<sup>−9</sup> for dicarbon phosphide (CCP) (Halfen et al. 2008), and an upper abundance of 3 × 10<sup>−8</sup> for the tentative detection of cyanophosphaethyne (NCCP) (Agúndez et al. 2014b). Furthermore, phosphaethyne (HCP) and phosphine (PH<sub>3</sub>) account for 5% and 2%, respectively, of the total phosphorus budget around IRC+10216 (Agúndez et al. 2014a). Given the carbon-rich nature of this circumstellar envelope, it is not surprising that four of the six phosphorus-bearing compounds around IRC+10216 also contain carbon. Using the phosphaethyne to hydrogen cyanide (HCN) ratio (HCP/HCN = 0.001, compared to the

solar ratio of 0.003) (Milam 2007) to estimate the phosphorus to nitrogen ratio, the relatively high abundance of nitrogen also rationalizes the presence of phosphorus nitride (PN) and cyanophosphaethyne (NCCP). Phosphorus monoxide (PO), on the other hand, was discovered in the oxygen-rich circumstellar envelope of the supergiant star VY Canis Majoris (Tenenbaum et al. 2007). Unlike phosphine, these molecules are notable in that phosphorus is bonded only to elements of the second period of the periodic table of the elements and that each compound contains a strong double or triple bond with phosphorus holding bond energies between 510 and 620 kJ mol<sup>−1</sup> (Johnson III 2015). In contrast, phosphine only contains phosphorus–hydrogen single bonds with a bond energy of only 343 kJ mol<sup>−1</sup> (Cottrell 1954).

It is not surprising that, with the exception of cyanophosphaethyne (NCCP), analogues to each of these compounds have been discovered in the interstellar medium in which phosphorus is substituted by its isovalent element: nitrogen. Given the discovery of phosphine, it follows that larger phosphorus-containing compounds analogous to those formed from isoelectronic ammonia should exist in interstellar environments. For example, methylamine (CH<sub>3</sub>NH<sub>2</sub>) was first discovered in the hot cores Sagittarius B2 and Orion A with abundances of 1 × 10<sup>−9</sup> and 3 × 10<sup>−9</sup>, respectively, compared to molecular hydrogen (Fourikis et al. 1974; Kaifu et al. 1974). Recent laboratory experiments exposing ices of ammonia (NH<sub>3</sub>) and C1 to C6 hydrocarbons (Kim & Kaiser 2011) to energetic electrons, which mimicked the interaction of secondary electrons generated in the track of galactic cosmic rays while penetrating ice-coated interstellar grains, demonstrated that methylamine (CH<sub>3</sub>NH<sub>2</sub>) can be

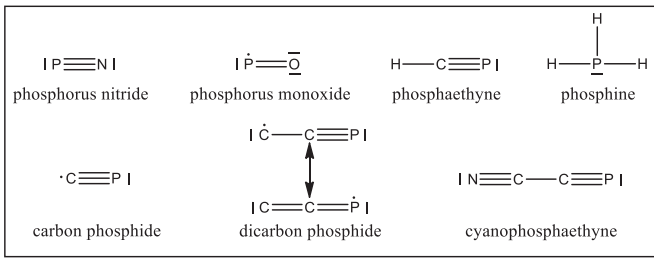


**Figure 1.** Phosphorus-bearing molecules detected in the interstellar medium.

formed via the barrierless recombination of methyl radicals ( $\text{CH}_3$ ) with amino radicals ( $\text{NH}_2$ ) at 10 K. If ammonia is replaced by phosphine, the phosphorus analogue, methylphosphine ( $\text{CH}_3\text{PH}_2$ ) is expected to form in interstellar analogue ices and predicted to exist toward Sagittarius B2 and Orion A along with methylamine (Lafont et al. 1982). However, as of today, interstellar methylphosphine ( $\text{CH}_3\text{PH}_2$ ) has remained elusive (Halfen et al. 2014). In the present work, we investigate to what extent carbon–phosphorus bond coupling can lead to the formation of methylphosphine ( $\text{CH}_3\text{PH}_2$ ) and potentially higher-order organophosphorus compounds in ices of phosphine ( $\text{PH}_3$ ) and methane ( $\text{CH}_4$ ) upon interaction with energetic electrons generated in the track of galactic cosmic ray particles penetrating ice-coated particles in cold molecular clouds.

## 2. EXPERIMENTAL

The experiments were conducted in a stainless steel chamber operating under ultra-high vacuum pressures of  $5 \times 10^{-11}$  Torr by exploiting oil-free turbomolecular pumps and dry scroll backing pumps (Bennett et al. 2013; Jones & Kaiser 2013; Jones et al. 2014a, 2014b; Kaiser et al. 2014, 2015; Maity et al. 2014a, 2014b, 2015; Maksyutenko et al. 2015). The ices were prepared on a reflective silver substrate mounted to a rotatable cold finger manufactured using oxygen-free high-conductivity copper capable of achieving temperatures as low as  $5.5 \pm 0.2$  K by a closed-cycle helium refrigerator (Sumitomo Heavy Industries, RDK-415E). Methane (Advanced Specialty Gases, 99.999%) and phosphine (Sigma-Aldrich, 99.9995%) were premixed in a gas mixing chamber at 110 Torr each and then introduced into the main recipient with the help of a glass capillary at a pressure of  $5 \times 10^{-8}$  Torr for 8 minutes. A Nicolet 6700 Fourier Transform Infrared Spectrometer (FTIR) probed the deposited ices on the silver substrate on line and in situ from  $6000 \text{ cm}^{-1}$  to  $500 \text{ cm}^{-1}$  with  $4 \text{ cm}^{-1}$  resolution, and the integrated infrared peak areas ( $\int_{\tilde{\nu}_1}^{\tilde{\nu}_2} A(\tilde{\nu}) d\tilde{\nu}$ ) of the  $\nu_2$  band of phosphine ( $987 \text{ cm}^{-1}$ ) and  $\nu_1 + \nu_4$  combination band of methane ( $4195 \text{ cm}^{-1}$ ) were used with their integrated absorption coefficients ( $A_{\text{exp}}$ ) of  $5.1 \times 10^{-19} \text{ cm molecule}^{-1}$  and  $3.5 \times 10^{-19} \text{ cm molecule}^{-1}$ , respectively (Brunetto et al. 2008; Turner et al. 2015), in the following equation to determine the column density ( $N$ ) of each reactant in the ice:

$$N = \frac{\ln(10) \int_{\tilde{\nu}_1}^{\tilde{\nu}_2} A(\tilde{\nu}) d\tilde{\nu}}{2 A_{\text{exp}}} \cos \left( \sin^{-1} \frac{\sin \alpha}{n_{\text{ice}}} \right). \quad (1)$$

The angle at which light passes through ice ( $\beta$ ) is related to the angle of the incoming beam ( $\alpha$ ) by Snell’s law:  $n_1 \sin \alpha = n_{\text{ice}} \sin \beta$ . This was incorporated into Equation (1) along

with a factor of 2 to account for the incoming and outgoing beams and by assigning the refractive index of vacuum to be  $n_1 = 1$ . To determine the refractive index of the ice mixture and the ice thickness, laser interferometry (Hudgins et al. 1993; Westley et al. 1998; Fulvio et al. 2009; Turner et al. 2015) was utilized during deposition by reflecting a helium–neon laser ( $\lambda = 632.8 \text{ nm}$ ) off the silver substrate and ice surfaces. The relative intensity between the maxima and minima of the interference fringes was used (Goodman 1978; Westley et al. 1998; Babar & Weaver 2015) to determine a refractive index of  $n_{\text{ice}} = 1.44 \pm 0.04$ , which ranges between the refractive indices of pure phosphine ( $n_{\text{PH}_3} = 1.51$ ) (Turner et al. 2015) and pure methane ( $n_{\text{CH}_4} = 1.33$ ) (Brunetto et al. 2008). The column densities of  $3.8 \pm 0.3 \times 10^{18}$  molecules  $\text{cm}^{-2}$  for phosphine and  $1.2 \pm 0.1 \times 10^{18}$  molecules  $\text{cm}^{-2}$  for methane indicate that the deposited ice mixture had a  $3.2 \pm 0.6:1.0$  phosphine to methane ratio. The ice thickness ( $d$ ) was measured using the equation:

$$d = \frac{m \lambda}{2 \sqrt{n_{\text{ice}}^2 - \sin^2 \theta}}. \quad (2)$$

Using the laser’s angle of incidence ( $\theta = 4^\circ \pm 1^\circ$ ) and by counting interference fringes ( $m = 4.45 \pm 0.05$  fringes),  $980 \pm 40 \text{ nm}$  of ice was deposited. One hour after the deposition, which was sufficient time to re-establish the base pressure, the ice was irradiated with 5 keV electrons at a flux of  $2 \times 10^{10}$  electrons  $\text{s}^{-1} \text{ cm}^{-2}$  at a  $70^\circ$  angle of incidence over an area of  $1.0 \pm 0.1 \text{ cm}^2$ . Monte Carlo (CASINO) (Hovington et al. 1997) calculations, which exploited the weighted averaged density of  $0.78 \text{ g cm}^{-3}$  from the phosphine ( $0.90 \text{ g cm}^{-3}$ ) (Francia & Nixon 1973; Turner et al. 2015) and methane ( $0.47 \text{ g cm}^{-3}$ ) (Satorre et al. 2008) densities, were performed and determined the average absorbed dose with a 540 nm average penetration depth to be  $3.5 \pm 0.4 \text{ eV molecule}^{-1}$  for phosphine and  $3.1 \pm 0.3 \text{ eV molecule}^{-1}$  for methane. Note that the penetration depth is smaller than the thickness of the ices indicating that the electrons only interact with the ices but not the silver substrate. A temperature programmed desorption (TPD) protocol heated the irradiated ice to 300 K with a heating rate of  $1 \text{ K minute}^{-1}$  and allowed the reactants and newly formed molecules to sublime. During the irradiation and heating, the FTIR monitored the ice on line and in situ. Also, two mass spectroscopic techniques analyzed the subliming species. A traditional quadrupole mass spectrometer (QMS) operating in residual gas analyzer (RGA) mode with 100 eV electrons at 1 mA emission current offered detection of molecules via electron impact ionization. A more sensitive reflectron time-of-flight (ReTOF) mass spectrometer (Jordan TOF Products, Inc.) utilizing single photon photo-ionization (118.2 nm, 10.49 eV) (Jones & Kaiser 2013) was also used. The pulsed (30 Hz) coherent vacuum ultraviolet (VUV) light was generated via four-wave mixing with xenon (99.999%) as the nonlinear medium. The third harmonic (354.6 nm) of a pulsed neodymium-doped yttrium aluminum garnet laser (Nd:YAG, Spectra Physics, PRO-250, 30 Hz) underwent a frequency tripling process ( $\omega_{\text{vuv}} = 3\omega_1$ ) to obtain the 118.2 nm light with about  $10^{14}$  photons per pulse (Maity

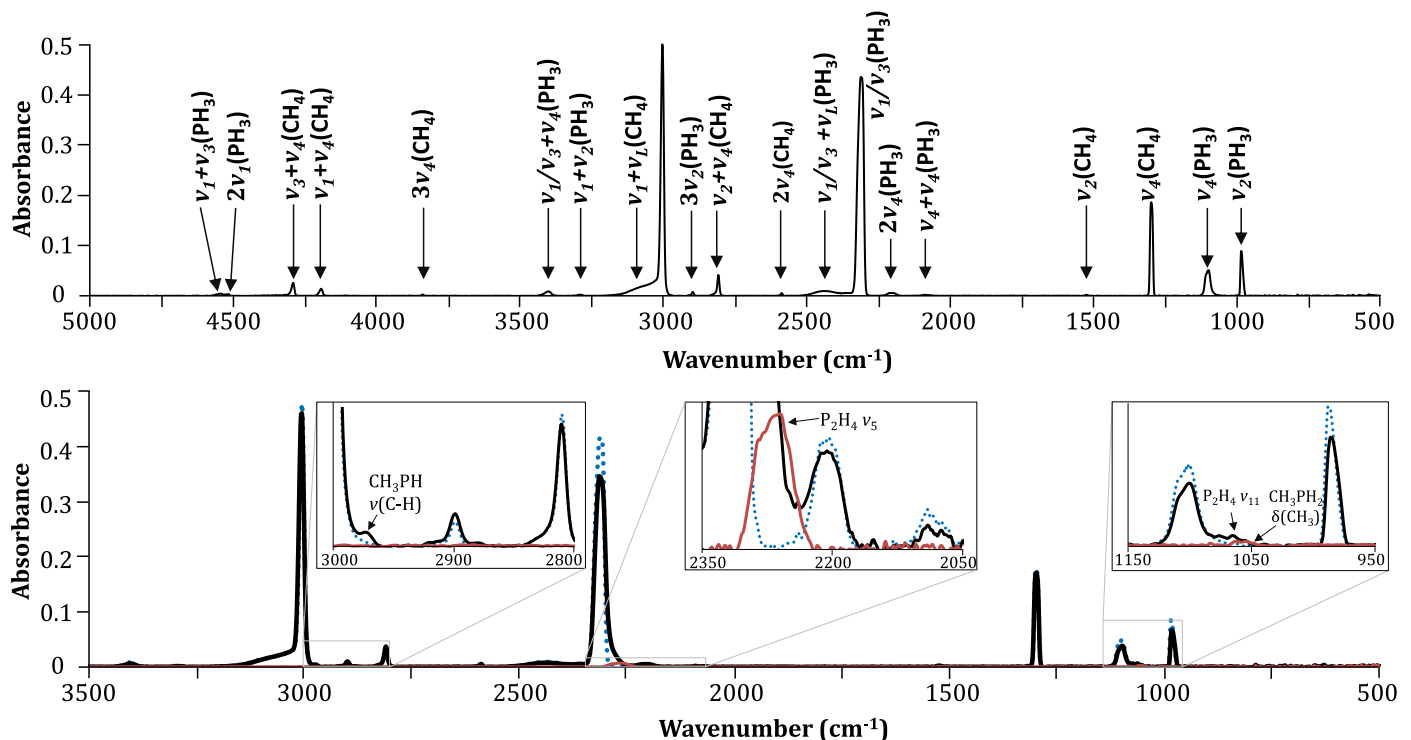


**Figure 2.** (Top) Infrared spectrum of pristine methane–phosphine ice at 5.5 K. (Bottom) Spectra of phosphine ( $\text{PH}_3$ ) and methane ( $\text{CH}_4$ ) ice before irradiation (blue dotted), after irradiation (black), and after methane and phosphine sublimed (90 K, red). New peaks seen from the irradiation are labeled.

et al. 2014b). This light was spatially separated from the fundamental using a lithium fluoride (LiF) planoconvex lens (VonDrasek et al. 1988) (ISP Optics, LF-PX-38-150) exploiting distinct refractive indices of LiF for different wavelengths of 1.40 and 1.59, respectively (Li 1976). The VUV light was directed 1 mm above the ice surface, and the photoionized molecules were mass analyzed with a ReTOF mass spectrometer. Here, the arrival time of the ions to a multichannel plate is based on the mass-to-charge ratio, and the signal was amplified with a fast preamplifier (Ortec 9305) and recorded with a bin width of 4 ns triggered at 30 Hz (Quantum Composers, 9518). Previous studies (Turner et al. 2015) have shown that the ionization energy of phosphanes range from 9.8 eV for  $\text{PH}_3$  to 7.5 eV for  $\text{P}_8\text{H}_{10}$ , and thus the chosen photon energy (10.49 eV) is capable of ionizing each of the phosphanes to be observed. Also, methylphosphine ( $\text{CH}_3\text{PH}_2$ ) ionizes at 9.1 eV (Staley & Beauchamp 1974; Hodges et al. 1980), and following trends of both phosphanes and alkanes that ionization energies decline with increasing molecular size, more complex alkylphosphanes are also expected to have ionization energies below 10.49 eV. To obtain mechanistic information, additional experiments were performed replacing methane with deuterated methane,  $\text{CD}_4$  (CDN Isotopes, 99.9% D atom) under otherwise identical experimental conditions.

### 3. RESULTS

#### 3.1. Infrared Spectroscopy

During the irradiation, infrared spectra were recorded in two-minute intervals (Figure 2 and Table 1). Most notably, the strong phosphorus–hydrogen stretching modes of phosphine

( $\text{PH}_3$ ) ( $\nu_1$  and  $\nu_3$ ) centered around  $2310 \text{ cm}^{-1}$  decreased and broadened due to the appearance of the  $\nu_5$  mode of diphosphine ( $\text{P}_2\text{H}_4$ ) ( $2262$  and  $2287 \text{ cm}^{-1}$ ). Also, the  $\nu_{11}$  mode of  $\text{P}_2\text{H}_4$  emerged, albeit more subtly, at  $1063 \text{ cm}^{-1}$  (Durig et al. 1996). Nearby, a tenuous peak at  $1054 \text{ cm}^{-1}$  was assigned to the deformation band of the methyl group in methylphosphine ( $\text{CH}_3\text{PH}_2$ ) (Kim et al. 2007), while a more distinguishable peak appears at  $2973 \text{ cm}^{-1}$  caused by carbon–hydrogen stretching. Thus, only four new peaks emerged during irradiation and only two products, diphosphine and methylphosphine, could be assigned. A drawback of using infrared spectroscopy for methane-doped phosphine ices is that the most intense vibrations, the phosphorus–hydrogen stretching mode, occur in the same region of the spectrum for all products, i.e., typically from  $2350$  to  $2250 \text{ cm}^{-1}$ . In addition, carbon–hydrogen stretching modes cannot be used to identify individual methylated phosphanes because the group frequencies overlap among each other in the range of  $3000$ – $2950 \text{ cm}^{-1}$ . After the sublimation of methane and phosphine (80 K), only the phosphorus–hydrogen stretches centered around  $2295 \text{ cm}^{-1}$  had significant intensity. Even after diphosphine sublimed (135 K), this peak slowly decreased in intensity and disappeared into the baseline as higher order products sublimed.

#### 3.2. Reflectron Time-of-flight Mass Spectrometry (ReTOF)

##### 3.2.1. Phosphanes

The ReTOF data using a 10.49 eV photoionization energy provided the most useful and ample results for determining the products of irradiated ices of phosphine ( $\text{PH}_3$ ) and methane ( $\text{CH}_4$ ) (Figure 3, Tables 2 and 3), especially when compared to quadrupole mass spectrometry results (Appendix). This highly

**Table 1**Infrared Absorption Assignments for Phosphine (PH<sub>3</sub>) and Methane (CH<sub>4</sub>) Ice at 5.5 K and the Irradiation Products

Assignment	Compound	Position (cm <sup>-1</sup> )	References
$\nu_2$	PH <sub>3</sub>	983, 987	(1)
$\nu_4$	PH <sub>3</sub>	1099, 1100, 1110sh	(1)
$\nu_4$	CH <sub>4</sub>	1296, 1302	(2)
$\nu_2$	CH <sub>4</sub>	1526	(2)
$\nu_2 + \nu_4$	PH <sub>3</sub>	2071, 2091	(1)
$2\nu_4$	PH <sub>3</sub>	2193, 2209	(1)
$\nu_1$	PH <sub>3</sub>	2305	(1)
$\nu_3$	PH <sub>3</sub>	2313, 2326	(1)
$\nu_1/\nu_3 + \nu_L$	PH <sub>3</sub>	2349, 2440, 2461	(1)
$2\nu_4$	CH <sub>4</sub>	2589	(2)
$\nu_2 + \nu_4$	CH <sub>4</sub>	2809, 2816	(2)
$3\nu_2$	PH <sub>3</sub>	2899	(1)
$\nu_3$	CH <sub>4</sub>	3002, 3006, 3008	(2)
$\nu_3 + \nu_L$	CH <sub>4</sub>	3029, 3074	(2)
$\nu_1 + \nu_2$	PH <sub>3</sub>	3293	(1)
$\nu_1 + \nu_4$	PH <sub>3</sub>	3402	(1)
$\nu_3 + \nu_4$	PH <sub>3</sub>	3420	(1)
$3\nu_4$	CH <sub>4</sub>	3841	(2)
$\nu_1 + \nu_4$	CH <sub>4</sub>	4193, 4198	(2)
$\nu_3 + \nu_4$	CH <sub>4</sub>	4291, 4296, 4306	(2)
$2\nu_1$	PH <sub>3</sub>	4519	(1)
$\nu_1 + \nu_3$	PH <sub>3</sub>	4547	(1)
New Peaks From Irradiation			
$\delta(\text{CH}_3)$	CH <sub>3</sub> PH <sub>2</sub>	1054	(3)
$\nu_{11}$	P <sub>2</sub> H <sub>4</sub>	1063	(4)
$\nu_5$	P <sub>2</sub> H <sub>4</sub>	2262, 2287	(4)
$\nu(\text{C-H})$	CH <sub>3</sub> PH <sub>2</sub>	2973	(3)

**Note.**  $\nu_L$  defines the lattice mode.

**References.** (1) Turner et al. (2015), (2) Bennett et al. (2006), (3) Kim et al. (2007), (4) Durig et al. (1996).

sensitive technique allowed molecular identification exploiting unique mass-to-charge ratios and well-defined sublimation temperatures from heating the ices to 300 K at a rate of 1 K minute<sup>-1</sup>. Figure 4 depicts the ion count intensity for methane-doped phosphine ice as a function of temperature during warm-up of the irradiated ices to 300 K at all mass-to-charge ratios observed in the ReTOF. A few observations consistent with the irradiation of pure phosphine ice (Turner et al. 2015) can be highlighted. First, a series of saturated phosphanes including diphosphine (P<sub>2</sub>H<sub>4</sub>), triphosphane (P<sub>3</sub>H<sub>5</sub>), tetraphosphane (P<sub>4</sub>H<sub>6</sub>), and pentaphosphane (P<sub>5</sub>H<sub>7</sub>) were observed at progressively increasing sublimation temperatures via their parent ions that peaked at 130 K, 162 K, 190 K, and 208 K, respectively. Furthermore, the molecular ion counts for P<sub>2</sub>H<sub>4</sub> and P<sub>3</sub>H<sub>5</sub> were by far the highest of any product. Diphosphine showed no evidence of fragmentation, while triphosphane fragmented mostly into PH<sub>4</sub><sup>+</sup> at a third of the parent ion intensity and also to minor amounts of P<sub>2</sub>H<sub>3</sub><sup>+</sup> and P<sub>2</sub>H<sub>2</sub><sup>+</sup> through PH<sub>2</sub> and PH<sub>3</sub> loss. Beginning with P<sub>4</sub>H<sub>6</sub>, fragmentation became dominant and the parent ion was about five times less intense than the combined major PH<sub>2</sub> and PH<sub>3</sub> loss fragments: P<sub>3</sub>H<sub>4</sub><sup>+</sup> and P<sub>3</sub>H<sub>3</sub><sup>+</sup>. Pentaphosphane (P<sub>5</sub>H<sub>7</sub>) showed that the extent of fragmentation increased with molecular size as the parent ion intensity was only 10% that of the PH<sub>2</sub> loss fragment, P<sub>4</sub>H<sub>5</sub><sup>+</sup>. A minor but notable protonated two-phosphorus fragment, P<sub>2</sub>H<sub>5</sub><sup>+</sup>, also occurred

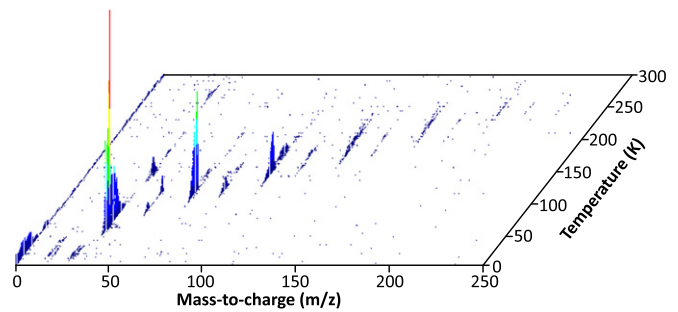


**Figure 3.** ReTOF mass spectrometry data as a function of sublimation temperature as irradiated phosphine (PH<sub>3</sub>) and methane (CH<sub>4</sub>) ice was heated from 5.5 K to 300 K at 1 K minute<sup>-1</sup>.

**Table 2**Observed Ions in the ReTOF Mass Spectrometer for the Phosphine (PH<sub>3</sub>) and Methane (CH<sub>4</sub>) Irradiation

Mass	Formula	Comments	Molecular Formula of Parent Compound
35	PH <sub>4</sub> <sup>+</sup>	fragment	P <sub>3</sub> H <sub>5</sub> , P <sub>4</sub> H <sub>6</sub> , CH <sub>3</sub> P <sub>4</sub> H <sub>5</sub>
48	CH <sub>3</sub> PH <sub>2</sub> <sup>+</sup>	parent	CH <sub>3</sub> PH <sub>2</sub>
49	<sup>13</sup> CH <sub>3</sub> PH <sub>2</sub> <sup>+</sup>	isotope	CH <sub>3</sub> PH <sub>2</sub>
	CH <sub>3</sub> PH <sub>3</sub> <sup>+</sup>	fragment	CH <sub>3</sub> P <sub>3</sub> H <sub>4</sub> , CH <sub>3</sub> P <sub>4</sub> H <sub>5</sub>
66	P <sub>2</sub> H <sub>4</sub> <sup>+</sup>	parent	P <sub>2</sub> H <sub>4</sub>
67	P <sub>2</sub> H <sub>5</sub> <sup>+</sup>	protonated parent	P <sub>2</sub> H <sub>4</sub>
		fragment	P <sub>4</sub> H <sub>6</sub> , P <sub>5</sub> H <sub>7</sub>
78	CH <sub>3</sub> P <sub>2</sub> H <sup>+</sup>	fragment	CH <sub>3</sub> P <sub>3</sub> H <sub>4</sub>
79	CH <sub>3</sub> P <sub>2</sub> H <sub>2</sub> <sup>+</sup>	fragment	CH <sub>3</sub> P <sub>3</sub> H <sub>4</sub>
80	CH <sub>3</sub> P <sub>2</sub> H <sub>3</sub> <sup>+</sup>	parent	CH <sub>3</sub> P <sub>2</sub> H <sub>3</sub>
81	<sup>13</sup> CH <sub>3</sub> P <sub>2</sub> H <sub>3</sub> <sup>+</sup>	isotope	CH <sub>3</sub> P <sub>2</sub> H <sub>3</sub>
	CH <sub>3</sub> P <sub>2</sub> H <sub>4</sub> <sup>+</sup>	fragment	CH <sub>3</sub> P <sub>5</sub> H <sub>6</sub>
96	P <sub>3</sub> H <sub>3</sub> <sup>+</sup>	fragment	P <sub>4</sub> H <sub>6</sub>
97	P <sub>3</sub> H <sub>4</sub> <sup>+</sup>	fragment	P <sub>4</sub> H <sub>6</sub>
98	P <sub>3</sub> H <sub>5</sub> <sup>+</sup>	parent	P <sub>3</sub> H <sub>5</sub>
99	P <sub>3</sub> H <sub>6</sub> <sup>+</sup>	protonated parent	P <sub>3</sub> H <sub>5</sub>
		fragment	P <sub>6</sub> H <sub>8</sub>
110	CH <sub>3</sub> P <sub>3</sub> H <sub>2</sub> <sup>+</sup>	fragment	CH <sub>3</sub> P <sub>4</sub> H <sub>5</sub>
111	CH <sub>3</sub> P <sub>3</sub> H <sub>3</sub> <sup>+</sup>	fragment	CH <sub>3</sub> P <sub>4</sub> H <sub>5</sub>
112	CH <sub>3</sub> P <sub>3</sub> H <sub>4</sub> <sup>+</sup>	parent	CH <sub>3</sub> P <sub>3</sub> H <sub>4</sub>
126	P <sub>4</sub> H <sub>2</sub> <sup>+</sup>	fragment	P <sub>6</sub> H <sub>8</sub>
127	P <sub>4</sub> H <sub>3</sub> <sup>+</sup>	fragment	P <sub>6</sub> H <sub>8</sub>
128	P <sub>4</sub> H <sub>4</sub> <sup>+</sup>	fragment	P <sub>6</sub> H <sub>8</sub>
129	P <sub>4</sub> H <sub>5</sub> <sup>+</sup>	fragment	P <sub>5</sub> H <sub>7</sub>
130	P <sub>4</sub> H <sub>6</sub> <sup>+</sup>	parent	P <sub>4</sub> H <sub>6</sub>
143	CH <sub>3</sub> P <sub>4</sub> H <sub>4</sub> <sup>+</sup>	fragment	CH <sub>3</sub> P <sub>5</sub> H <sub>6</sub>
144	CH <sub>3</sub> P <sub>4</sub> H <sub>5</sub> <sup>+</sup>	parent	CH <sub>3</sub> P <sub>4</sub> H <sub>5</sub>
159	P <sub>5</sub> H <sub>4</sub> <sup>+</sup>	fragment	P <sub>6</sub> H <sub>8</sub> , P <sub>7</sub> H <sub>9</sub>
160	P <sub>5</sub> H <sub>5</sub> <sup>+</sup>	fragment	P <sub>6</sub> H <sub>8</sub> , P <sub>7</sub> H <sub>9</sub>
161	P <sub>5</sub> H <sub>6</sub> <sup>+</sup>	fragment	P <sub>6</sub> H <sub>8</sub>
162	P <sub>5</sub> H <sub>7</sub> <sup>+</sup>	parent	P <sub>5</sub> H <sub>7</sub>
175	CH <sub>3</sub> P <sub>5</sub> H <sub>5</sub> <sup>+</sup>	fragment	CH <sub>3</sub> P <sub>6</sub> H <sub>7</sub>
191	P <sub>6</sub> H <sub>5</sub> <sup>+</sup>	fragment	P <sub>7</sub> H <sub>9</sub> , P <sub>8</sub> H <sub>10</sub>
193	P <sub>6</sub> H <sub>7</sub> <sup>+</sup>	fragment	P <sub>7</sub> H <sub>9</sub>
207	CH <sub>3</sub> P <sub>6</sub> H <sub>6</sub> <sup>+</sup>	fragment	CH <sub>3</sub> P <sub>7</sub> H <sub>8</sub>
225	P <sub>7</sub> H <sub>8</sub> <sup>+</sup>	fragment	P <sub>8</sub> H <sub>10</sub>
239	CH <sub>3</sub> P <sub>7</sub> H <sub>7</sub> <sup>+</sup>	fragment	CH <sub>3</sub> P <sub>8</sub> H <sub>9</sub>

for P<sub>5</sub>H<sub>7</sub>. Starting with hexaphosphane (P<sub>6</sub>H<sub>8</sub>), fragmentation was quantitative so that the molecular ion could no longer be observed in the mass spectra, making P<sub>5</sub>H<sub>7</sub><sup>+</sup> the largest observed parent ion. However, given the sequential order of sublimation temperatures as phosphanes increase in size along with the predictable pattern of fragmentation—predominantly

**Table 3**  
Fragmentation Patterns and Onset Sublimation Temperatures of Product Molecules for Phosphine (PH<sub>3</sub>) with Methane (CH<sub>4</sub>) Irradiation

Compound	Sublimation Temperature	Species Detected by ReTOF-MS	Ratio of Species Detected (Scaled to 100)
CH <sub>3</sub> PH <sub>2</sub>	87 K	CH <sub>3</sub> PH <sub>2</sub> <sup>+</sup>	100
P <sub>2</sub> H <sub>4</sub>	98 K	P <sub>2</sub> H <sub>5</sub> <sup>+</sup> , P <sub>2</sub> H <sub>4</sub> <sup>+</sup>	0.75:100
CH <sub>3</sub> P <sub>2</sub> H <sub>3</sub>	118 K	CH <sub>3</sub> P <sub>2</sub> H <sub>3</sub> <sup>+</sup>	100
P <sub>3</sub> H <sub>5</sub>	131 K	P <sub>3</sub> H <sub>6</sub> <sup>+</sup> , P <sub>3</sub> H <sub>5</sub> <sup>+</sup> , PH <sub>4</sub> <sup>+</sup>	0.3:100:34
CH <sub>3</sub> P <sub>3</sub> H <sub>4</sub>	148 K	CH <sub>3</sub> P <sub>3</sub> H <sub>4</sub> <sup>+</sup> , CH <sub>3</sub> P <sub>2</sub> H <sub>2</sub> <sup>+</sup> , CH <sub>3</sub> P <sub>2</sub> H <sup>+</sup> , CH <sub>3</sub> PH <sub>3</sub> <sup>+</sup>	100:53:31:4
P <sub>4</sub> H <sub>6</sub>	160 K	P <sub>4</sub> H <sub>6</sub> <sup>+</sup> , P <sub>3</sub> H <sub>4</sub> <sup>+</sup> , P <sub>3</sub> H <sub>3</sub> <sup>+</sup> , P <sub>2</sub> H <sub>5</sub> <sup>+</sup> , PH <sub>4</sub> <sup>+</sup>	35:85:100:2:12
CH <sub>3</sub> P <sub>4</sub> H <sub>5</sub>	175 K	CH <sub>3</sub> P <sub>4</sub> H <sub>5</sub> <sup>+</sup> , CH <sub>3</sub> P <sub>3</sub> H <sub>3</sub> <sup>+</sup> , CH <sub>3</sub> P <sub>3</sub> H <sub>2</sub> <sup>+</sup> , CH <sub>3</sub> PH <sub>3</sub> <sup>+</sup>	29:100:16:7
P <sub>5</sub> H <sub>7</sub>	185 K	P <sub>5</sub> H <sub>7</sub> <sup>+</sup> , P <sub>4</sub> H <sub>5</sub> <sup>+</sup> , P <sub>4</sub> H <sub>4</sub> <sup>+</sup> , P <sub>2</sub> H <sub>5</sub> <sup>+</sup>	10:100:40:10
CH <sub>3</sub> P <sub>5</sub> H <sub>6</sub>	197 K	CH <sub>3</sub> P <sub>4</sub> H <sub>4</sub> <sup>+</sup> , CH <sub>3</sub> P <sub>2</sub> H <sub>4</sub> <sup>+</sup>	100:10
P <sub>6</sub> H <sub>8</sub>	206 K	P <sub>5</sub> H <sub>6</sub> <sup>+</sup> , P <sub>5</sub> H <sub>5</sub> <sup>+</sup> , P <sub>5</sub> H <sub>4</sub> <sup>+</sup> , P <sub>4</sub> H <sub>3</sub> <sup>+</sup> , P <sub>4</sub> H <sub>2</sub> <sup>+</sup> , P <sub>3</sub> H <sub>6</sub> <sup>+</sup>	100:9:7:23:15:6
CH <sub>3</sub> P <sub>6</sub> H <sub>7</sub>	218 K	CH <sub>3</sub> P <sub>5</sub> H <sub>5</sub> <sup>+</sup>	100
P <sub>7</sub> H <sub>9</sub>	231 K	P <sub>6</sub> H <sub>7</sub> <sup>+</sup> , P <sub>6</sub> H <sub>5</sub> <sup>+</sup> , P <sub>5</sub> H <sub>5</sub> <sup>+</sup> , P <sub>5</sub> H <sub>4</sub> <sup>+</sup>	100:17:10:31
CH <sub>3</sub> P <sub>7</sub> H <sub>8</sub>	243 K	CH <sub>3</sub> P <sub>6</sub> H <sub>6</sub> <sup>+</sup>	100
P <sub>8</sub> H <sub>10</sub>	252 K	P <sub>7</sub> H <sub>8</sub> <sup>+</sup> , P <sub>6</sub> H <sub>5</sub> <sup>+</sup>	100:85
CH <sub>3</sub> P <sub>8</sub> H <sub>9</sub>	264 K	CH <sub>3</sub> P <sub>7</sub> H <sub>7</sub> <sup>+</sup>	100

**Note.** Because molecular ions for products larger than P<sub>5</sub>H<sub>7</sub> and CH<sub>3</sub>P<sub>4</sub>H<sub>5</sub> were not observed, fragments were utilized to determine sublimation temperatures. The ratios of observed species assigned to each product are listed to illustrate the fragmentation patterns

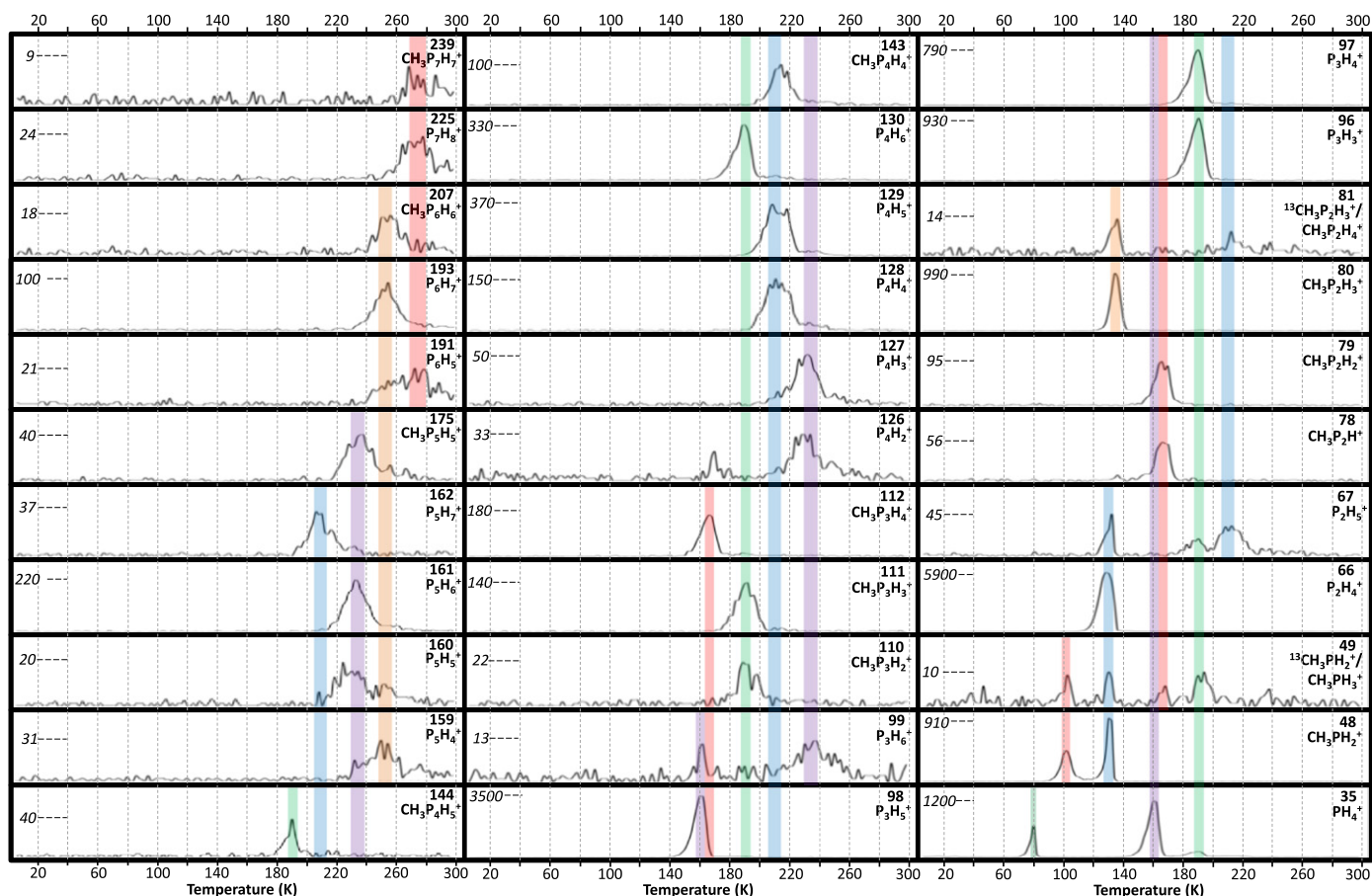


**Figure 4.** Time-of-flight mass spectra for the products of phosphine (PH<sub>3</sub>) and methane (CH<sub>4</sub>) irradiation as a function of temperature. Colored bands indicate sublimation events at similar temperatures. The intensity is listed on the left of each spectrum, while the mass-to-charge and ionic formula is on the right.

from PH<sub>2</sub> loss—fragments can be used to infer the presence of their parent compounds (Figure 4). Specifically, the intensity and sublimation temperature of fragment ions P<sub>5</sub>H<sub>6</sub><sup>+</sup>, P<sub>6</sub>H<sub>7</sub><sup>+</sup>, and P<sub>7</sub>H<sub>8</sub><sup>+</sup> was exploited as a proxy for determination of hexaphosphane (P<sub>6</sub>H<sub>8</sub>), heptaphosphane (P<sub>7</sub>H<sub>9</sub>), and octaphosphane (P<sub>8</sub>H<sub>10</sub>). In summary, phosphine in the irradiated

phosphine–methane ice reacted to form saturated phosphanes as complex as P<sub>8</sub>H<sub>10</sub>.

### 3.2.2. Organophosphorus Molecules

Further analysis revealed that each of the phosphanes observed in the ReTOF also correlated with an associated

methylphosphane of the generic molecular formula  $\text{CH}_3\text{P}_x\text{H}_{x+1}$ , with  $x = 1-8$ . The most abundant products were molecules with the formula  $\text{CH}_3\text{PH}_2$  and  $\text{CH}_3\text{P}_2\text{H}_3$ , which occurred in similar quantities, although  $\text{CH}_3\text{PH}_2$  had two distinct sublimation events, which was unique among products, at 102 and 130 K. The first event was exploited to determine the onset sublimation temperature for methylphosphine ( $\text{CH}_3\text{PH}_2$ ), while the second peak occurred coincidentally with diphosphine ( $\text{P}_2\text{H}_4$ ) sublimation. Here, a significant portion of  $\text{CH}_3\text{PH}_2$  remained trapped in the  $\text{P}_2\text{H}_4$  matrix, which was the most abundant product, and was released when  $\text{P}_2\text{H}_4$  sublimated. Neither  $\text{CH}_3\text{PH}_2$  nor  $\text{CH}_3\text{P}_2\text{H}_3$  showed evidence of fragmentation. However, considering the next member, nearly half of the sublimed  $\text{CH}_3\text{P}_3\text{H}_4$  fragmented into  $\text{CH}_3\text{P}_2\text{H}_2^+$  and  $\text{CH}_3\text{P}_2\text{H}^+$ , which result from  $\text{PH}_2$  and  $\text{PH}_3$  loss. The heaviest molecular ion observed for methylphosphanes was  $\text{CH}_3\text{P}_4\text{H}_5$ , and the combined  $\text{PH}_2$  and  $\text{PH}_3$  loss fragments from  $\text{CH}_3\text{P}_4\text{H}_5$  had a 4:1 ratio compared to the parent ion. All methylphosphanes including  $\text{CH}_3\text{P}_4\text{H}_5$  and larger sublimated at similar temperatures as their non-methylated phosphane analogues, which complicates fragmentation analysis because  $\text{P}_3\text{H}_3^+$  and  $\text{P}_3\text{H}_4^+$  could be fragments from both  $\text{CH}_3\text{P}_4\text{H}_5$  and  $\text{P}_4\text{H}_6$ . However, given the observed ratios of  $\text{P}_2\text{H}_4^+$  to  $\text{CH}_3\text{P}_2\text{H}_3^+$  (6:1) and  $\text{P}_3\text{H}_5^+$  to  $\text{CH}_3\text{P}_3\text{H}_4^+$  (20:1), it is likely that  $\text{P}_4\text{H}_6$  formed in larger amounts than  $\text{CH}_3\text{P}_4\text{H}_5$  and thus the  $\text{P}_3\text{H}_4^+$  and  $\text{P}_3\text{H}_3^+$  fragments originated predominately from  $\text{P}_4\text{H}_6$ , which itself had a parent ion ratio of 8:1 with  $\text{CH}_3\text{P}_4\text{H}_5^+$ . The parent ion for  $\text{CH}_3\text{P}_5\text{H}_6$  was not observed, which is not surprising given the previously stated ratios between phosphanes and their methylated equivalents and that the intensity of  $\text{P}_5\text{H}_7^+$  was diminished due to increased fragmentation. However,  $\text{CH}_3\text{P}_5\text{H}_6$  can still be detected since it sublimated at a similar peak temperature of 212 K as  $\text{P}_5\text{H}_7$  and the major  $\text{PH}_2$  loss fragment,  $\text{CH}_3\text{P}_4\text{H}_4^+$ , was easily observed. This method also worked for the larger methylphosphanes  $\text{CH}_3\text{P}_6\text{H}_7$ ,  $\text{CH}_3\text{P}_7\text{H}_8$ , and  $\text{CH}_3\text{P}_8\text{H}_9$ , which were identified using their fragments from  $\text{PH}_2$  loss that appeared concurrently with the fragments from  $\text{P}_6\text{H}_8$ ,  $\text{P}_7\text{H}_9$ , and  $\text{P}_8\text{H}_{10}$ , respectively. Thus, the irradiated methane-phosphine ices produced a series of phosphanes from  $\text{P}_2\text{H}_4$  to  $\text{P}_8\text{H}_{10}$  and methylated phosphanes from  $\text{CH}_3\text{PH}_2$  to  $\text{CH}_3\text{P}_8\text{H}_9$ . Notably, neither alkylphosphanes more complex than methylphosphanes nor pure hydrocarbons were detected, which was likely a result of the three-to-one phosphine-to-methane ratio in the ice mixture.

While the larger phosphanes showed similar *peak* sublimation temperatures with their methylated analogues, the temperature at the *onset* of sublimation was distinct. Figure 5 and Table 3 show how onset sublimation temperatures increase with atomic weight and how, from  $\text{PH}_3$  to  $\text{P}_8\text{H}_{10}$  and from  $\text{CH}_3\text{PH}_2$  to  $\text{CH}_3\text{P}_8\text{H}_9$ , the amount of temperature increase declined with each successive member in the series. For  $\text{PH}_3$  to  $\text{P}_3\text{H}_5$ , the onset sublimation temperatures were 17–20 K lower than their corresponding methylated form: 69 K versus 87 K for  $\text{PH}_3/\text{CH}_3\text{PH}_2$ , 98 K versus 118 K for  $\text{P}_2\text{H}_4/\text{CH}_3\text{P}_2\text{H}_3$ , and 131 K versus 148 K for  $\text{P}_3\text{H}_5/\text{CH}_3\text{P}_3\text{H}_4$ . The  $\text{P}_4\text{H}_6/\text{CH}_3\text{P}_4\text{H}_5$  pair had a slightly lower difference of 15 K at 160 K versus 175 K, while  $\text{P}_5\text{H}_8$  (185 K),  $\text{P}_6\text{H}_8$  (206 K),  $\text{P}_7\text{H}_9$  (231 K), and  $\text{P}_8\text{H}_{10}$  (252 K) each began sublimating 12 K below their methylated forms. Since higher order products were not observed via their parent ions, the fragments discussed previously were utilized to determine the onset sublimation temperature of the parent. The regression curves in Figure 5 used only the temperatures for

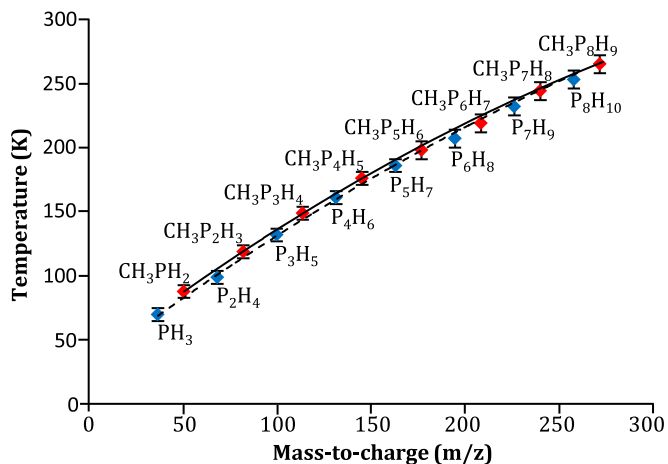


Figure 5. Onset sublimation temperatures for the phosphanes (blue) and alkylphosphanes (red) observed in the ReTOF mass spectrometer.

directly observed ions, i.e.,  $\text{PH}_3$  through  $\text{P}_5\text{H}_7$  and  $\text{CH}_3\text{PH}_2$  through  $\text{CH}_3\text{P}_4\text{H}_5$ , and the curves were fit forward to higher order compounds. The regression curves show good agreement with the assignments of parent ions from their fragments, which support the use of fragments when the intensity of parent ions is below the detection limit.

These ReTOF findings are consistent with the results when  $\text{CH}_4$  was substituted with  $\text{CD}_4$  in the phosphine ices (Figure 6 and Table 4) with the highest observed molecular ions at  $m/z = 147$  ( $\text{CD}_3\text{P}_4\text{H}_5^+$ ) and  $162$  ( $\text{P}_5\text{H}_7^+$ ). Using the fragments at  $m/z = 210$  ( $\text{CD}_3\text{P}_6\text{H}_6^+$ ) and  $225$  ( $\text{P}_8\text{H}_{10}^+$ ), we inferred the largest products formed in these ices were  $\text{CD}_3\text{P}_7\text{H}_8$  and  $\text{P}_8\text{H}_{10}$ . However, additional mass-to-charge ratios appear associated with the various isotopologues of the methylphosphanes. For example with the simplest product, methylphosphine ( $\text{CH}_3\text{PH}_2$ ), three isotopologues appeared in a 2:10:1 ratio:  $m/z = 50$  ( $\text{CHD}_2\text{PH}_2$ ), 51 ( $\text{CD}_3\text{PH}_3$ ), and 52 ( $\text{CD}_3\text{PHD}$ ). Section 4.2 discusses these results in detail.

## 4. ANALYSIS

### 4.1. Quantitative Analysis—Mass Balance

Although the infrared results provide limited information about the identity of the products, the significant changes in the area of the reactant peaks glean information about the amount of reactants destroyed and the rate of these reactions. Figure 7 compiles the column densities of phosphine and methane during irradiation with an energy flux of  $10^{14}$  eV  $\text{cm}^{-2}$   $\text{s}^{-1}$  utilizing the infrared peaks at  $987$   $\text{cm}^{-1}$  and  $4195$   $\text{cm}^{-1}$  with integrated absorption coefficients of  $5.1 \times 10^{-19}$   $\text{cm molecule}^{-1}$  and  $3.5 \times 10^{-19}$   $\text{cm molecule}^{-1}$  (Brunetto et al. 2008; Turner et al. 2015). These column densities were fitted with the following first order rate equations:

$$[\text{PH}_3]_t = [\text{PH}_3]_{t=0} e^{-k_1 t} \quad (3)$$

$$[\text{CH}_4]_t = [\text{CH}_4]_{t=0} e^{-k_2 t}. \quad (4)$$

The rate at which phosphine and methane react are described by the rate constants  $k_1 = 4.7 \pm 0.2 \times 10^{-5}$   $\text{s}^{-1}$  and  $k_2 = 3.8 \pm 1.7 \times 10^{-5}$   $\text{s}^{-1}$ . In pure phosphine ices, the rate constant for the destruction of phosphine leading to the formation of diphosphine, which accounted for  $89 \pm 4\%$  of the products, was found to be  $k = 4.8 \pm 0.1 \times 10^{-5}$   $\text{s}^{-1}$ ,

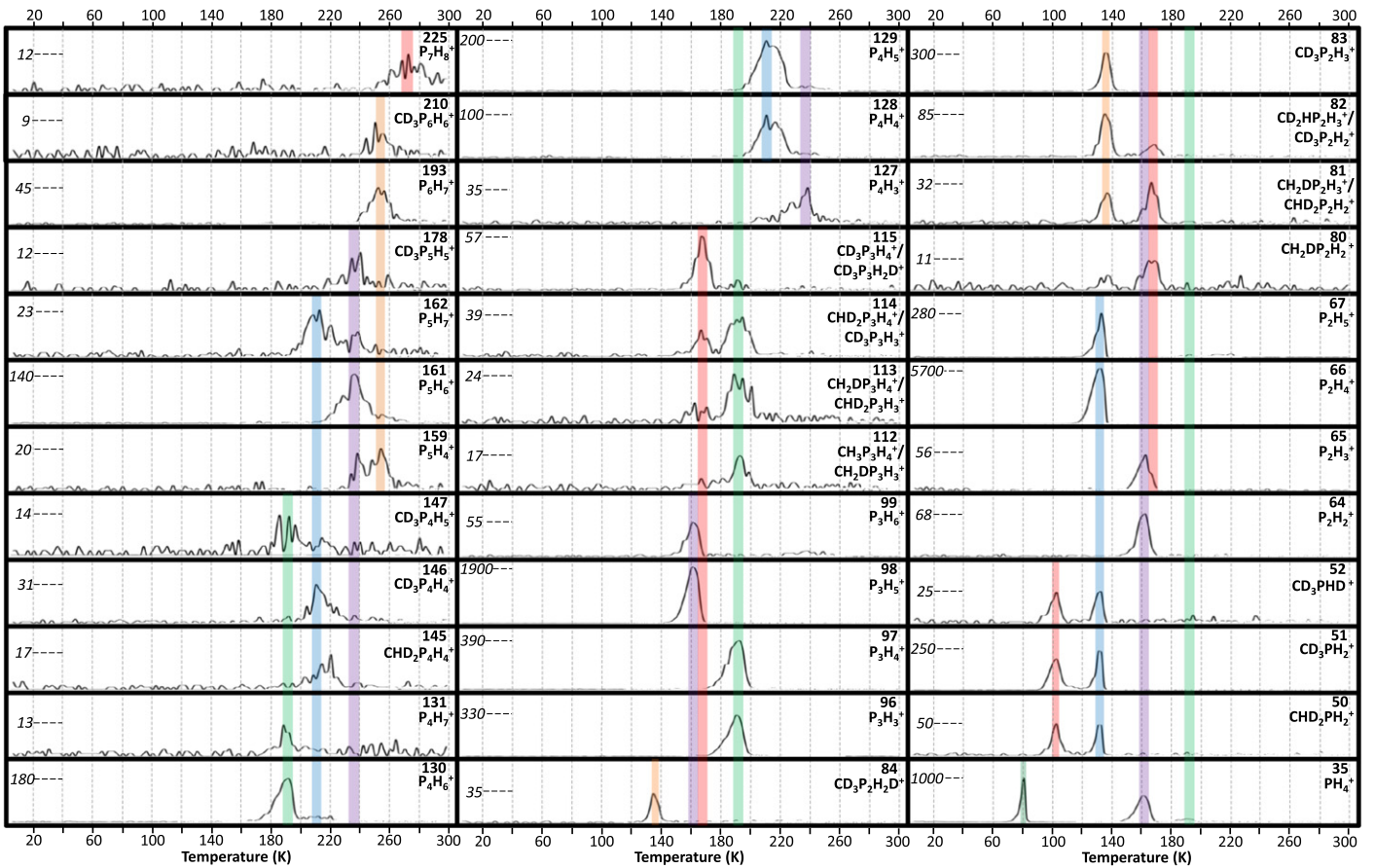


**Figure 6.** Reflectron time-of-flight mass spectra for phosphine ( $\text{PH}_3$ ) and deuterated methane ( $\text{CD}_4$ ) irradiation. Colored bands indicate sublimation events at similar temperatures. The intensity is listed on the left of each spectrum, while the mass-to-charge and ionic formula is on the right.

which is in agreement with the rate of destruction of phosphine in phosphine–methane ices.

In total,  $6.4 \pm 1.6 \times 10^{17}$  molecules  $\text{cm}^{-2}$  of phosphine were destroyed, which is a  $17 \pm 4\%$  loss. A lower percentage of the initial methane reacted,  $13 \pm 5\%$ , which is equivalent to  $1.6 \pm 0.6 \times 10^{17}$  molecules  $\text{cm}^{-2}$ . This resulted in a loss rate of  $0.11 \pm 0.03$  molecules  $\text{eV}^{-1}$  for phosphine and  $0.09 \pm 0.03$  molecules  $\text{eV}^{-1}$  for methane. Since the  $\nu_{11}$  band of diphosphine at  $1063 \text{ cm}^{-1}$  grew too subtly and was partially overlapped by the  $\nu_4$  band of phosphine, the temporal profile of diphosphine could not be monitored. However, the before- and after-irradiation spectra were compared to calculate this peak area and estimate the total diphosphine production. Using an integrated absorption coefficient of  $7.0 \times 10^{-19} \text{ cm molecule}^{-1}$  (Turner et al. 2015),  $1.6 \pm 0.4 \times 10^{17}$  molecules  $\text{cm}^{-2}$  of diphosphine were produced. Thus, diphosphine accounted for  $50 \pm 13\%$  of the phosphorus from phosphine destruction. Given that the irradiated ice had a three-to-one phosphine-to-methane ratio and that diphosphine contained 89% of the reacted phosphorus in pure phosphine ices, proportionally less diphosphine was formed in phosphine–methane ices, which indicates that either phosphine or diphosphine readily reacts with methane.

## 4.2. Reaction Pathways

### 4.2.1. Methylphosphine

The ReTOF results from irradiated phosphine and deuterated methane ice provide crucial information regarding the

mechanism of formation for methylphosphanes by analyzing the intensities of various isotopologues. Figure 8 shows the possible formation routes that would lead to each of the three observed isotopologues of methylphosphine ( $\text{CH}_3\text{PH}_2$ ). To obtain  $m/z = 50$  ( $\text{CHD}_2\text{PH}_2$ ),  $\text{CD}_4$  has to decompose via the loss of molecular hydrogen or two deuterium atoms to form carbene ( $\text{CD}_2$ ), which has been observed in previous irradiated ice studies (Holtom et al. 2005; Bennett & Kaiser 2007), and then insert into a phosphorus–hydrogen bond of phosphine (reaction (5)). If the carbene is formed in its first excited singlet state ( $a^1A_1$ ), the insertion is barrierless (Gordon et al. 1987). For  $m/z = 51$  ( $\text{CD}_3\text{PH}_2$ ), methane and phosphine each lost a hydrogen or deuterium atom, and the resulting methyl ( $\text{CD}_3$ ) (Kaiser et al. 1997) and phosphino ( $\text{PH}_2$ ) radicals recombined barrierlessly (reaction (6)). Finally, the formation of  $m/z = 52$  ( $\text{CD}_3\text{PHD}$ ) mirrors that for  $\text{CHD}_2\text{PH}_2$  but in this case phosphine lost two hydrogen atoms or molecular hydrogen to create the phosphinidene ( $\text{PH}$ ) radical and then inserted into a carbon–deuterium bond of methane (reaction (7)). Phosphinidene, like imidogen ( $\text{NH}$ ) (Fueno et al. 1983), is expected to insert barrierlessly in its first excited singlet state ( $a^1\Delta$ ):

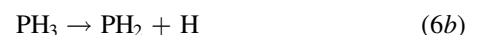
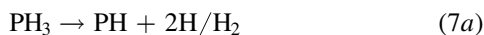


**Table 4**Observed Ions in the ReTOF Mass Spectrometer for the Phosphine (PH<sub>3</sub>) and Deuterated Methane (CD<sub>4</sub>) Irradiation

Mass	Formula	Comments	Formula of Parent Compound
35	PH <sub>4</sub> <sup>+</sup>	fragment	P <sub>3</sub> H <sub>5</sub> , P <sub>4</sub> H <sub>6</sub> , CD <sub>3</sub> P <sub>4</sub> H <sub>5</sub>
50	CHD <sub>2</sub> PH <sub>2</sub> <sup>+</sup>	parent	CHD <sub>2</sub> PH <sub>2</sub>
51	CD <sub>3</sub> PH <sub>2</sub> <sup>+</sup>	parent	CD <sub>3</sub> PH <sub>2</sub>
52	CD <sub>3</sub> PHD <sup>+</sup>	parent	CD <sub>3</sub> PHD
64	P <sub>2</sub> H <sub>2</sub> <sup>+</sup>	fragment	P <sub>3</sub> H <sub>5</sub>
65	P <sub>2</sub> H <sub>3</sub> <sup>+</sup>	fragment	P <sub>3</sub> H <sub>5</sub>
66	P <sub>2</sub> H <sub>4</sub> <sup>+</sup>	parent	P <sub>2</sub> H <sub>4</sub>
67	P <sub>2</sub> H <sub>5</sub> <sup>+</sup>	protonated parent fragment	P <sub>2</sub> H <sub>4</sub> P <sub>5</sub> H <sub>7</sub>
81	CH <sub>2</sub> DP <sub>2</sub> H <sub>3</sub> <sup>+</sup>	parent	CH <sub>2</sub> DP <sub>2</sub> H <sub>3</sub>
	CHD <sub>2</sub> P <sub>2</sub> H <sub>2</sub> <sup>+</sup>	fragment	CHD <sub>2</sub> P <sub>3</sub> H <sub>4</sub>
82	CHD <sub>2</sub> P <sub>2</sub> H <sub>3</sub> <sup>+</sup>	parent	CHD <sub>2</sub> P <sub>2</sub> H <sub>3</sub>
	CD <sub>3</sub> P <sub>2</sub> H <sub>2</sub> <sup>+</sup>	fragment	CD <sub>3</sub> P <sub>3</sub> H <sub>4</sub>
83	CD <sub>3</sub> P <sub>2</sub> H <sub>3</sub> <sup>+</sup>	parent	CD <sub>3</sub> P <sub>2</sub> H <sub>3</sub>
84	CD <sub>3</sub> P <sub>2</sub> H <sub>2</sub> D <sup>+</sup>	parent	CD <sub>3</sub> P <sub>2</sub> H <sub>2</sub> D
96	P <sub>3</sub> H <sub>3</sub> <sup>+</sup>	fragment	P <sub>4</sub> H <sub>6</sub>
97	P <sub>3</sub> H <sub>4</sub> <sup>+</sup>	fragment	P <sub>4</sub> H <sub>6</sub>
98	P <sub>3</sub> H <sub>5</sub> <sup>+</sup>	parent	P <sub>3</sub> H <sub>5</sub>
99	P <sub>3</sub> H <sub>6</sub> <sup>+</sup>	protonated parent	P <sub>3</sub> H <sub>5</sub>
111	CH <sub>3</sub> P <sub>3</sub> H <sub>3</sub> <sup>+</sup>	fragment	CH <sub>3</sub> P <sub>4</sub> H <sub>5</sub>
112	CH <sub>3</sub> P <sub>3</sub> H <sub>4</sub> <sup>+</sup>	parent	CH <sub>3</sub> P <sub>3</sub> H <sub>4</sub>
	CH <sub>2</sub> DP <sub>3</sub> H <sub>3</sub> <sup>+</sup>	fragment	CH <sub>2</sub> DP <sub>4</sub> H <sub>5</sub>
113	CH <sub>2</sub> DP <sub>3</sub> H <sub>4</sub> <sup>+</sup>	parent	CH <sub>2</sub> DP <sub>3</sub> H <sub>4</sub>
	CHD <sub>2</sub> P <sub>3</sub> H <sub>3</sub> <sup>+</sup>	fragment	CHD <sub>2</sub> P <sub>4</sub> H <sub>5</sub>
114	CHD <sub>2</sub> P <sub>3</sub> H <sub>4</sub> <sup>+</sup>	parent	CHD <sub>2</sub> P <sub>3</sub> H <sub>4</sub>
	CD <sub>3</sub> P <sub>3</sub> H <sub>3</sub> <sup>+</sup>	fragment	CD <sub>3</sub> P <sub>4</sub> H <sub>5</sub>
115	CD <sub>3</sub> P <sub>3</sub> H <sub>4</sub> <sup>+</sup>	parent	CD <sub>3</sub> P <sub>3</sub> H <sub>4</sub>
	CD <sub>3</sub> P <sub>3</sub> H <sub>2</sub> D <sup>+</sup>	fragment	CD <sub>3</sub> P <sub>4</sub> H <sub>4</sub> D
126	P <sub>4</sub> H <sub>2</sub> <sup>+</sup>	fragment	P <sub>6</sub> H <sub>8</sub>
127	P <sub>4</sub> H <sub>3</sub> <sup>+</sup>	fragment	P <sub>6</sub> H <sub>8</sub>
128	P <sub>4</sub> H <sub>4</sub> <sup>+</sup>	fragment	P <sub>5</sub> H <sub>7</sub> , P <sub>6</sub> H <sub>8</sub>
129	P <sub>4</sub> H <sub>5</sub> <sup>+</sup>	fragment	P <sub>5</sub> H <sub>7</sub> , P <sub>6</sub> H <sub>8</sub>
130	P <sub>4</sub> H <sub>6</sub> <sup>+</sup>	parent fragment	P <sub>4</sub> H <sub>6</sub> P <sub>5</sub> H <sub>7</sub>
131	P <sub>4</sub> H <sub>7</sub> <sup>+</sup>	protonated parent fragment	P <sub>4</sub> H <sub>6</sub> P <sub>5</sub> H <sub>7</sub>
145	CHD <sub>2</sub> P <sub>4</sub> H <sub>4</sub> <sup>+</sup>	fragment	CHD <sub>2</sub> P <sub>5</sub> H <sub>6</sub>
146	CD <sub>3</sub> P <sub>4</sub> H <sub>4</sub> <sup>+</sup>	fragment	CD <sub>3</sub> P <sub>5</sub> H <sub>6</sub>
147	CD <sub>3</sub> P <sub>4</sub> H <sub>5</sub> <sup>+</sup>	parent	CD <sub>3</sub> P <sub>4</sub> H <sub>5</sub>
159	P <sub>5</sub> H <sub>4</sub> <sup>+</sup>	fragment	P <sub>6</sub> H <sub>8</sub> , P <sub>7</sub> H <sub>9</sub>
160	P <sub>5</sub> H <sub>5</sub> <sup>+</sup>	fragment	P <sub>6</sub> H <sub>8</sub>
161	P <sub>5</sub> H <sub>6</sub> <sup>+</sup>	fragment	P <sub>6</sub> H <sub>8</sub>
162	P <sub>5</sub> H <sub>7</sub> <sup>+</sup>	parent fragment	P <sub>5</sub> H <sub>7</sub> P <sub>6</sub> H <sub>8</sub>
177	CHD <sub>2</sub> P <sub>5</sub> H <sub>5</sub> <sup>+</sup>	fragment	CHD <sub>2</sub> P <sub>6</sub> H <sub>7</sub> <sup>+</sup>
178	CD <sub>3</sub> P <sub>5</sub> H <sub>5</sub> <sup>+</sup>	fragment	CD <sub>3</sub> P <sub>6</sub> H <sub>7</sub> <sup>+</sup>
193	P <sub>6</sub> H <sub>7</sub> <sup>+</sup>	fragment	P <sub>6</sub> H <sub>8</sub>
210	CD <sub>3</sub> P <sub>6</sub> H <sub>6</sub> <sup>+</sup>	fragment	CD <sub>3</sub> P <sub>7</sub> H <sub>8</sub>
225	P <sub>7</sub> H <sub>8</sub> <sup>+</sup>	fragment	P <sub>8</sub> H <sub>10</sub> <sup>+</sup>



Therefore, our results provide compelling evidence that methane decomposes not only to the methyl radical, but also to carbene. Likewise, phosphine was found to fragment to the phosphino radical and also to phosphinidene. The ratio of ion intensities for  $m/z = 50:51:52$  is 2:10:1, indicating that radical recombination was the preferred formation pathway with

**Table 5**Observed Ions in the Quadrupole Mass Spectrometer for the Phosphine (PH<sub>3</sub>) and Methane (CH<sub>4</sub>) Irradiation

Mass	Formula	Comments	Formula of Parent Compound
35	PH <sub>4</sub> <sup>+</sup>	fragment	P <sub>3</sub> H <sub>5</sub>
48	CH <sub>3</sub> PH <sub>2</sub> <sup>+</sup>	parent	CH <sub>3</sub> PH <sub>2</sub>
62	P <sub>2</sub> <sup>+</sup>	fragment	P <sub>2</sub> H <sub>4</sub>
63	P <sub>2</sub> H <sup>+</sup>	fragment	P <sub>2</sub> H <sub>4</sub>
64	P <sub>2</sub> H <sub>2</sub> <sup>+</sup>	fragment	P <sub>2</sub> H <sub>4</sub>
65	P <sub>2</sub> H <sub>3</sub> <sup>+</sup>	fragment	P <sub>2</sub> H <sub>4</sub> , P <sub>3</sub> H <sub>5</sub>
66	P <sub>2</sub> H <sub>4</sub> <sup>+</sup>	parent	P <sub>2</sub> H <sub>4</sub>
80	CH <sub>3</sub> P <sub>2</sub> H <sub>3</sub> <sup>+</sup>	parent	CH <sub>3</sub> P <sub>2</sub> H <sub>3</sub>
93	P <sub>3</sub> <sup>+</sup>	fragment	P <sub>3</sub> H <sub>5</sub>
98	P <sub>3</sub> H <sub>5</sub> <sup>+</sup>	parent	P <sub>3</sub> H <sub>5</sub>

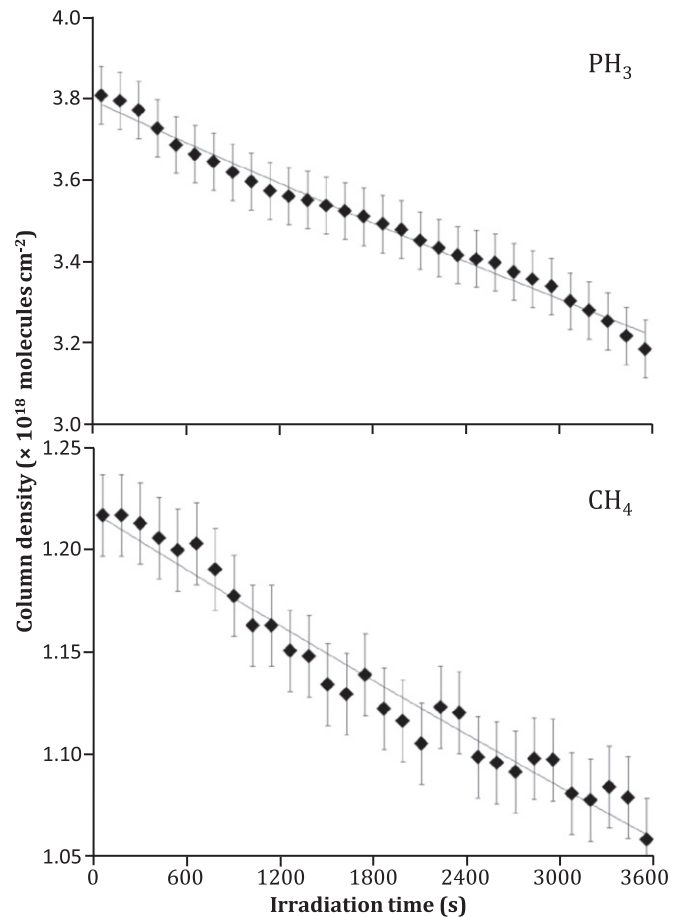


**Figure 7.** Column density of phosphine (top) and methane (bottom) as a function of irradiation time at  $10^{14}$  eV cm<sup>-2</sup> s<sup>-1</sup>.

CD<sub>3</sub>PH<sub>2</sub> as the most abundant isotopologue. This could either be a result of the methyl and phosphino radicals reacting quickly or that more of these radicals were produced than carbene and phosphinidene.

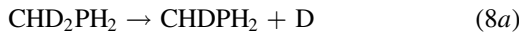
#### 4.2.2. Methylidiphosphine and Methyleneidiphosphine

The molecular formula CH<sub>6</sub>P<sub>2</sub> can have two structural isomers: the carbon-terminated methylidiphosphine (CH<sub>3</sub>P<sub>2</sub>H<sub>3</sub>) and the carbon-bridging methyleneidiphosphine (PH<sub>2</sub>CH<sub>2</sub>PH<sub>2</sub>). Figures 9 and 10 show the pathways by which each of these isomers could be formed using the intermediates from the

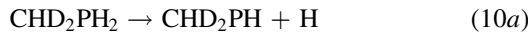
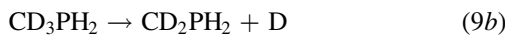
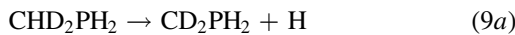
**Table 6**Observed Ions in the Quadrupole Mass Spectrometer for the Phosphine (PH<sub>3</sub>) and Deuterated Methane (CD<sub>4</sub>) Irradiation

Mass	Formula	Comments	Molecular Formula of Parent Compound
35	PH <sub>4</sub> <sup>+</sup>	fragment	P <sub>3</sub> H <sub>5</sub>
50	CHD <sub>2</sub> PH <sub>2</sub> <sup>+</sup>	parent	CHD <sub>2</sub> PH <sub>2</sub>
51	CD <sub>3</sub> PH <sub>2</sub> <sup>+</sup>	parent	CD <sub>3</sub> PH <sub>2</sub>
62	P <sub>2</sub> <sup>+</sup>	fragment	P <sub>2</sub> H <sub>4</sub>
63	P <sub>2</sub> H <sup>+</sup>	fragment	P <sub>2</sub> H <sub>4</sub>
64	P <sub>2</sub> H <sub>2</sub> <sup>+</sup>	fragment	P <sub>2</sub> H <sub>4</sub>
65	P <sub>2</sub> H <sub>3</sub> <sup>+</sup>	fragment	P <sub>2</sub> H <sub>4</sub> , P <sub>3</sub> H <sub>5</sub>
66	P <sub>2</sub> H <sub>4</sub> <sup>+</sup>	parent	P <sub>2</sub> H <sub>4</sub>
98	P <sub>3</sub> H <sub>5</sub> <sup>+</sup>	parent	P <sub>3</sub> H <sub>5</sub>

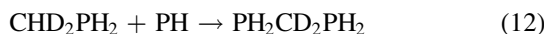
irradiation of methane, phosphine, and methylphosphine. From Section 4.2.1, it was shown that the isotopologues of methylphosphine were CHD<sub>2</sub>PH<sub>2</sub>, CD<sub>3</sub>PH<sub>2</sub>, and CD<sub>3</sub>PHD. Noting that non-deuterated CH<sub>6</sub>P<sub>2</sub> has  $m/z = 80$ , the observed peak at  $m/z = 81$  contained only one deuterium atom. Because the results in Section 4.2.1 indicate that the deuterated methylidyne radical (CD) was not formed, carbene (CD<sub>2</sub>) must be involved and methylphosphine (CHD<sub>2</sub>PH<sub>2</sub>) would first be formed by reaction (5). Reaction (8) shows that the loss of a deuterium atom from CHD<sub>2</sub>PH<sub>2</sub> formed the core one-deuterium radical compound that recombined with a phosphino radical (PH<sub>2</sub>) to form the methylenediphosphine isotopologue PH<sub>2</sub>CHDPH<sub>2</sub>. Given the starting materials and intermediates available, this is the only reaction pathway that can lead to  $m/z = 81$  and thus the presence of methylenediphosphine is explicitly confirmed:



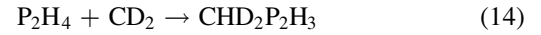
The signal for  $m/z = 82$  can be identified as three isotopomers (PH<sub>2</sub>CD<sub>2</sub>PH<sub>2</sub>, PHDCHDPH<sub>2</sub>, and CHD<sub>2</sub>P<sub>2</sub>H<sub>3</sub>) with two deuterium atoms that can be formed through several pathways. Each of the three can be formed using CHD<sub>2</sub>PH<sub>2</sub>. Hydrogen loss from either the carbon or phosphorus atom in CHD<sub>2</sub>PH<sub>2</sub> followed by recombination with the phosphino radical is shown in reaction (9) and reaction (10), respectively. Reaction (9) can also be completed by deuterium loss from CD<sub>3</sub>PH<sub>2</sub>:



Also, insertion pathways involving CHD<sub>2</sub>PH<sub>2</sub> are available in which the phosphinidene radical inserts into the phosphorus–hydrogen or carbon–phosphorus (reaction (11)) bond, the carbon–hydrogen bond (reaction (12)), or the carbon–deuterium bond (reaction (13)) of CHD<sub>2</sub>PH<sub>2</sub>:

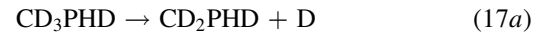
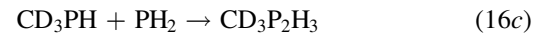
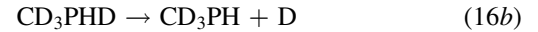


A final reaction that results in  $m/z = 82$  has carbene (CD<sub>2</sub>) inserting into a phosphorus–hydrogen (reaction (14)) or phosphorus–phosphorus bond (reaction (15)) of diphosphine:

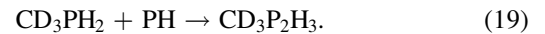


In summary,  $m/z = 82$  can be assigned to two isotopomers of *d*<sub>2</sub>-methylenediphosphine (PH<sub>2</sub>CD<sub>2</sub>PH<sub>2</sub> and PHDCHDPH<sub>2</sub>) and one isotopologue of methyl diphosphine (CHD<sub>2</sub>P<sub>2</sub>H<sub>3</sub>). We suggest that PH<sub>2</sub>CD<sub>2</sub>PH<sub>2</sub> through reaction (9b) is the most abundant contributor to  $m/z = 82$  because CD<sub>3</sub>PH<sub>2</sub> is the most abundant isotopologue of methylphosphine and phosphino radicals are readily available in irradiated phosphine-dominant ices.

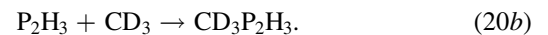
Two isomers can contribute to  $m/z = 83$ : one for methylenediphosphine (PHDCD<sub>2</sub>PH<sub>2</sub>) and another for methyl diphosphine (CD<sub>3</sub>P<sub>2</sub>H<sub>3</sub>). Irradiation of CD<sub>3</sub>PH<sub>2</sub> and CD<sub>3</sub>PHD followed by recombination with the phosphino radical can result in either of these isomers depending on which hydrogen or deuterium atom is lost. Reaction ((16a) and (16b)) shows hydrogen and deuterium loss from the phosphorus atom on CD<sub>3</sub>PH<sub>2</sub> and CD<sub>3</sub>PHD, respectively, and in reaction (17) the deuterium atom can be lost from carbon on CD<sub>3</sub>PHD:



The two isomers can also be formed via phosphinidene (PH) insertion into either a carbon–deuterium (reaction (18)) or a phosphorus–carbon/hydrogen (reaction (19)) bond of CD<sub>3</sub>PH<sub>2</sub>:



The final reaction mechanism (reaction (20)) involves the loss of a hydrogen atom from diphosphine (P<sub>2</sub>H<sub>4</sub>) and subsequent recombination with the methyl radical (CD<sub>3</sub>):



Thus, the methylphosphines CD<sub>3</sub>PH<sub>2</sub> and CD<sub>2</sub>PHD are capable of producing both methylenediphosphine and methyl diphosphine at  $m/z = 83$ , while diphosphine can only lead to methyl diphosphine. The dominant isotopomer is likely CD<sub>3</sub>P<sub>2</sub>H<sub>3</sub> as due to reaction (16a) and reaction (20). Not only are both radical recombination reactions, which have been shown to be the most favorable mechanism, but also reaction (16a) begins with the most abundant isotopologue of methylphosphine (CD<sub>3</sub>PH<sub>2</sub>), which then reacts with the radical from the most abundant reactant—the phosphino radical from phosphine. Similarly, reaction (20) shows the most abundant overall product, diphosphine, combining with a radical from the methane reactant.

Three isotopomers could be assigned to  $m/z = 84$ , and each originated from CD<sub>3</sub>PHD: PHDCD<sub>2</sub>PHD, CD<sub>3</sub>PDPH<sub>2</sub>, and CD<sub>3</sub>PHPHD. The insertion of the phosphinidene radical (PH) into a carbon–phosphorus bond or phosphorus–deuterium bond of CD<sub>3</sub>PHD is represented by reaction (21), while insertion into

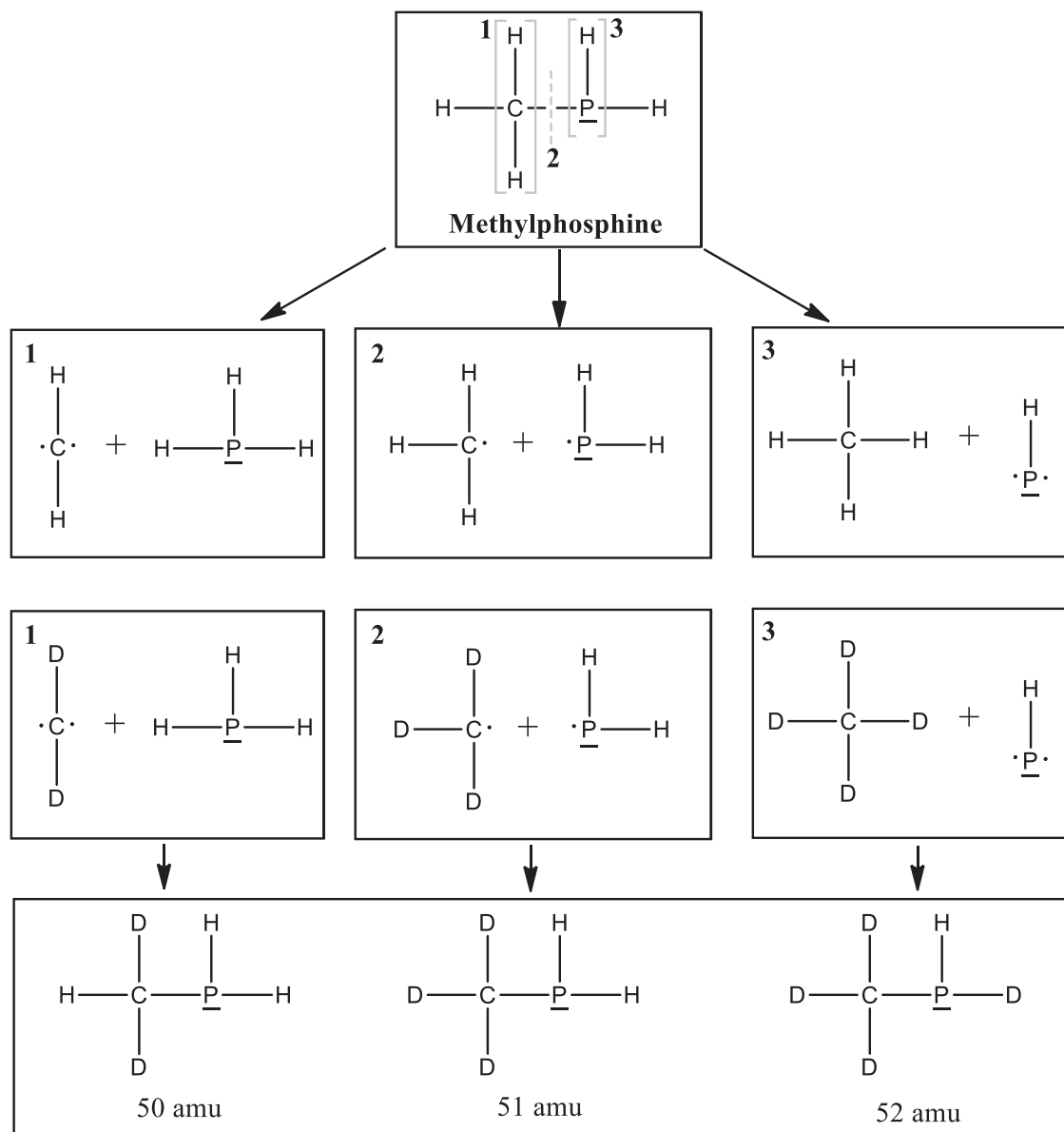
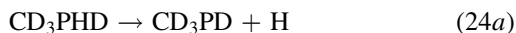


**Figure 8.** Retrosynthesis pathways from methylphosphine ( $\text{CH}_3\text{PH}_2$ ) identifying the possible formulae from deuterated-methane substituted reactions. The masses shown were observed in the ReTOF.

a carbon–deuterium or phosphorus–hydrogen bond is shown by reaction (22) and reaction (23), respectively:



Thus, phosphinidene insertion can explain each of the possible isotopomers. However, one radical recombination pathway is also possible by hydrogen loss from  $\text{CD}_3\text{PHD}$  followed by recombination with a phosphino radical (reaction (24)):



Reactions (21)–(24) provide little information about which product is most likely. While radical recombination has been previously identified as most probable, the low probability of

hydrogen being removed from  $\text{CD}_3\text{PHD}$  makes this reaction unlikely. A comparison of the PH-insertion pathways shows that reaction (22) has three bonds available for insertion, reaction (21) has two bonds, and reaction (23) can only occur by insertion into only one bond. Thus, without further information about the ease at which the phosphinidene radical can insert into various bond types,  $\text{PHDCD}_2\text{PHD}$  may be the most abundant product at  $m/z = 84$ .

#### 4.2.3. Summary

Some important conclusions from the irradiation of phosphine-deuterated methane ices are as follows.

First, the methylphosphine isotopologues have ratios for  $m/z = 50:51:52$  of 2:10:1, indicating that radical recombination ( $\text{CD}_3\text{PH}_2$ ) dominates and that carbene insertion ( $\text{CHD}_2\text{PH}_2$ ) is twice as likely as phosphinidene insertion ( $\text{CD}_3\text{PHD}$ ).

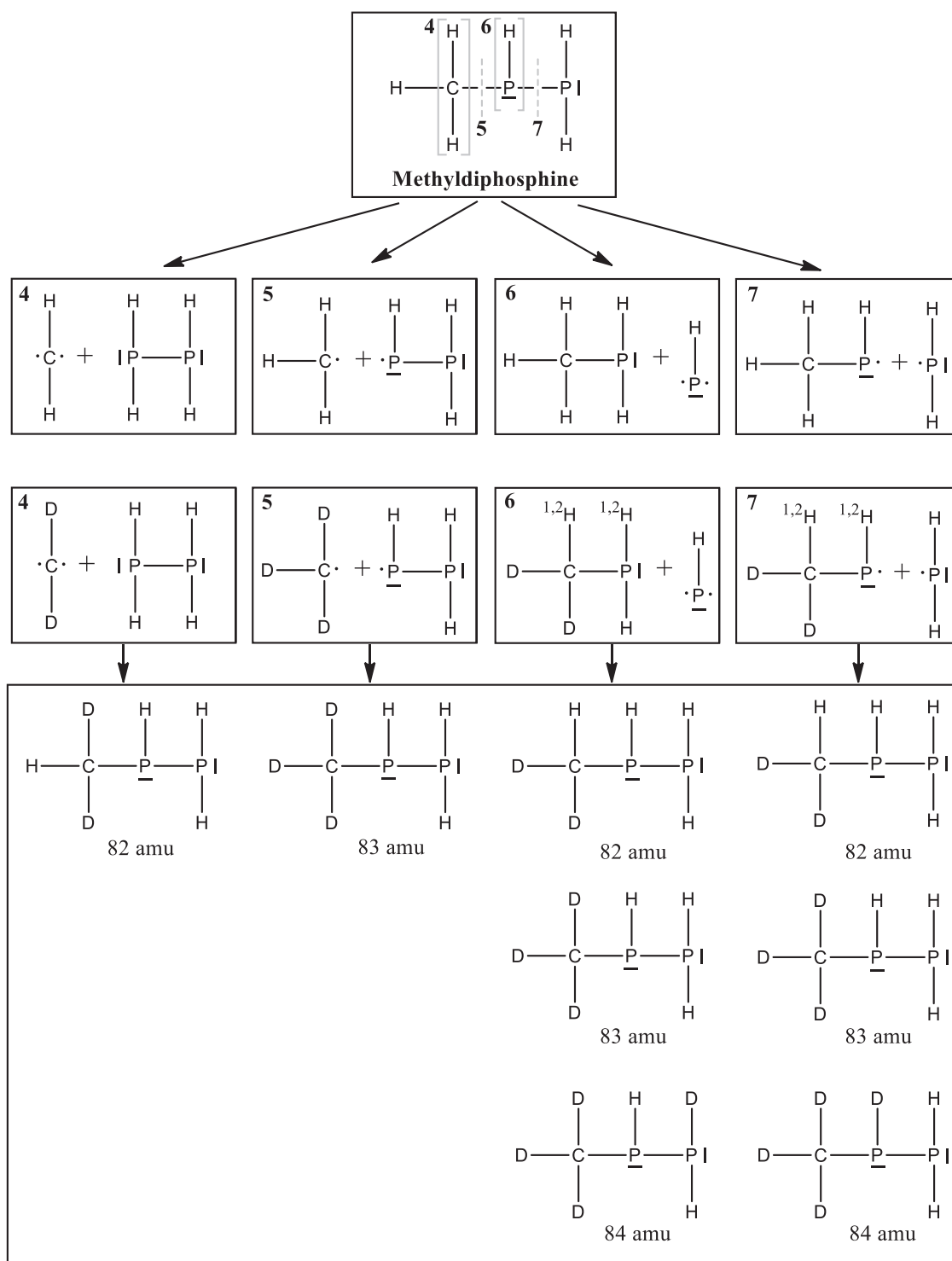


**Figure 9.** Retrosynthesis pathways from methylphosphine ( $\text{CH}_3\text{P}_2\text{H}_3$ ) identifying the possible formulae from deuterated-methane substituted reactions. The masses shown were observed in the ReTOF.

Second, the signals assigned to deuterated  $\text{CH}_6\text{P}_2$  have ratios for  $m/z = 80:81:82:83$  of 2:7:25:3. The most abundant product is thus  $\text{CD}_3\text{P}_2\text{H}_3$  (at  $m/z = 83$ ), which is formed by radical recombination of either  $\text{CD}_3\text{PH}$  with  $\text{PH}_2$  (reaction (16)) or  $\text{CD}_3$  with  $\text{P}_2\text{H}_3$  (reaction (20)).

Third, the signal at  $m/z = 81$  confirms that methylenediphosphine ( $\text{PH}_2\text{CHDPH}_2$ ) must be present and that it formed via radical recombination of  $\text{CHDPH}_2$  and  $\text{PH}_2$  starting from  $\text{CHD}_2\text{PH}_2$  and  $\text{PH}_3$  (reaction (8)). This provides further

evidence of the formation of  $\text{CHDPH}_2$  ( $m/z = 50$ ) via carbene insertion into a phosphorus–hydrogen bond of phosphine (reaction (5)).

Fourth, because the carbon–deuterium bond was cleaved in  $\text{CHD}_2\text{PH}_2$ , the decomposition of  $\text{CHD}_2\text{PH}_2$  should also result in hydrogen loss to give  $\text{CD}_2\text{PH}_2$ , which can then recombine with the phosphino radical to form  $\text{PH}_2\text{CD}_2\text{PH}_2$  ( $m/z = 82$ ). Furthermore, carbon–deuterium bond cleavage should similarly occur in  $\text{CD}_3\text{PH}_2$  and  $\text{CD}_3\text{PHD}$ , which when recombined with

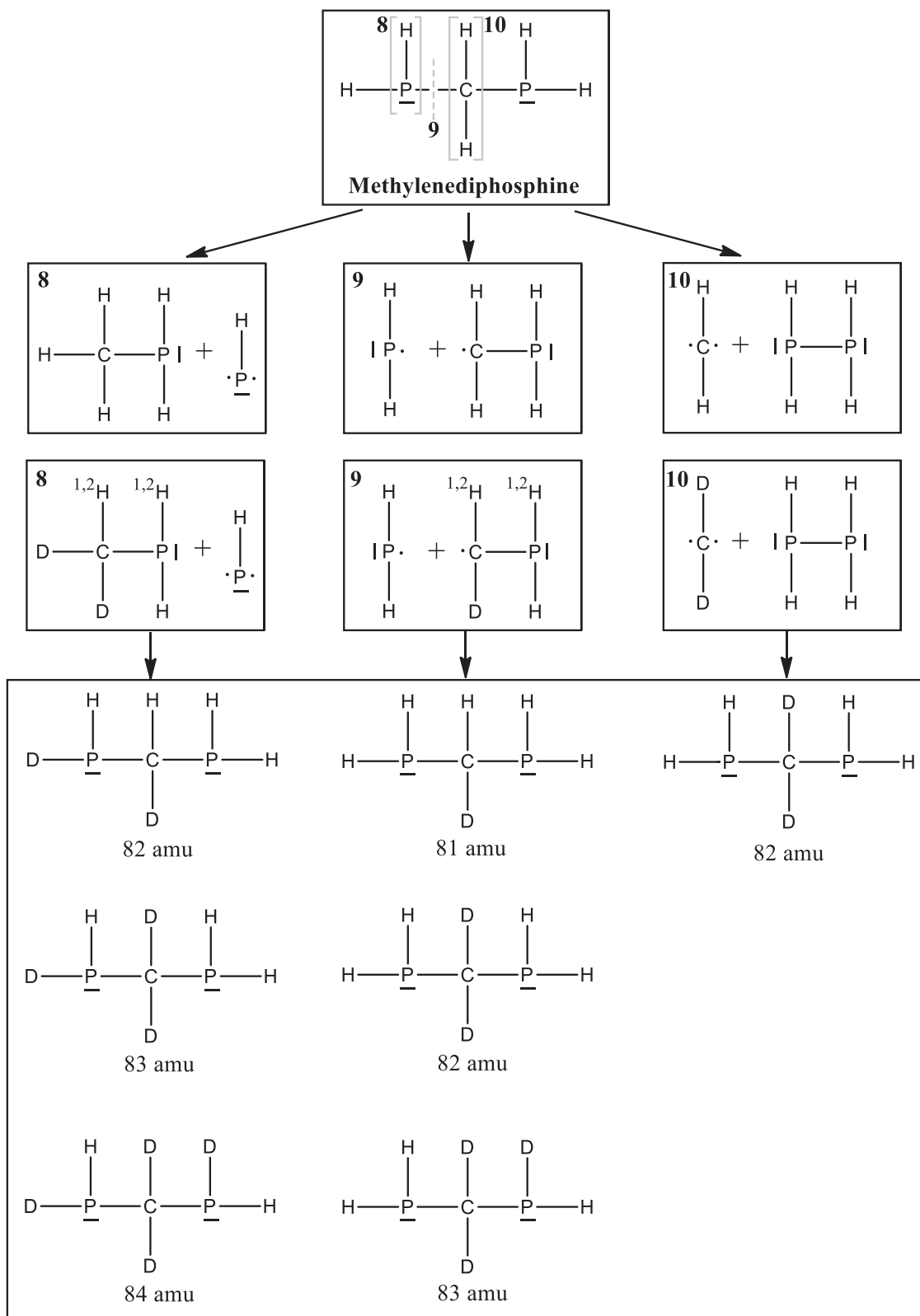


**Figure 10.** Retrosynthesis pathways from methylenediphosphine ( $\text{PH}_2\text{CH}_2\text{PH}_2$ ) identifying the possible structures from deuterated-methane substituted reactions. The masses shown were observed in the ReTOF.

the phosphino radical would also form  $\text{PH}_2\text{CD}_2\text{PH}_2$  ( $m/z = 82$ ) in greater abundance than  $\text{CHD}_2\text{PH}_2$  and also form  $\text{PHDCD}_2\text{PH}_2$  ( $m/z = 83$ ). Thus, compelling evidence exists for the formation three isotopologues of methylenediphosphine.

Fifth, all pathways forming  $m/z = 84$  require  $\text{CD}_3\text{PHD}$ , which not only confirms this isotopologue of methylphosphine but also provides evidence that the phosphinidene radical inserts into a carbon–deuterium bond of methane.

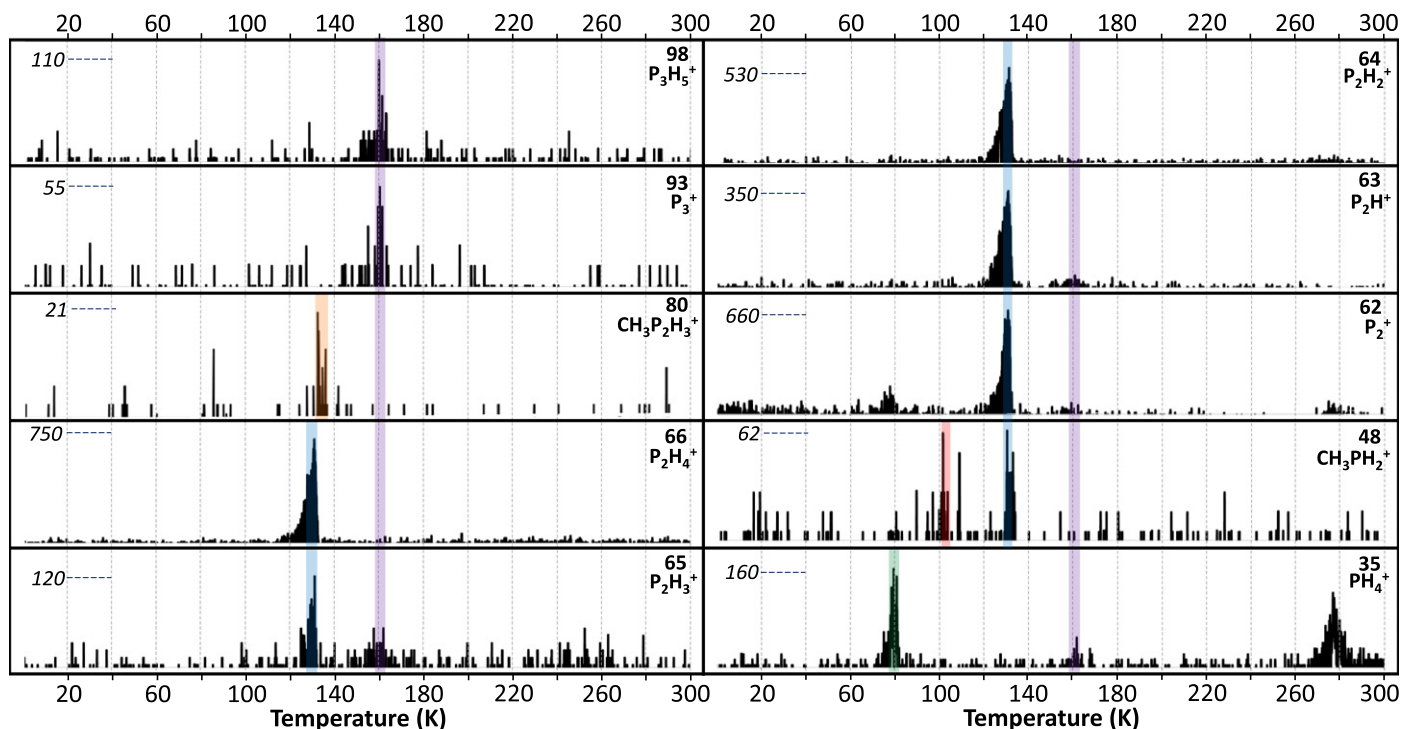


**Figure 11.** Quadrupole mass spectra of the products from phosphine ( $\text{PH}_3$ ) and methane ( $\text{CH}_4$ ) irradiation. The intensity (in thousands) is listed on the left while the mass-to-charge and ionic formula are on the right.

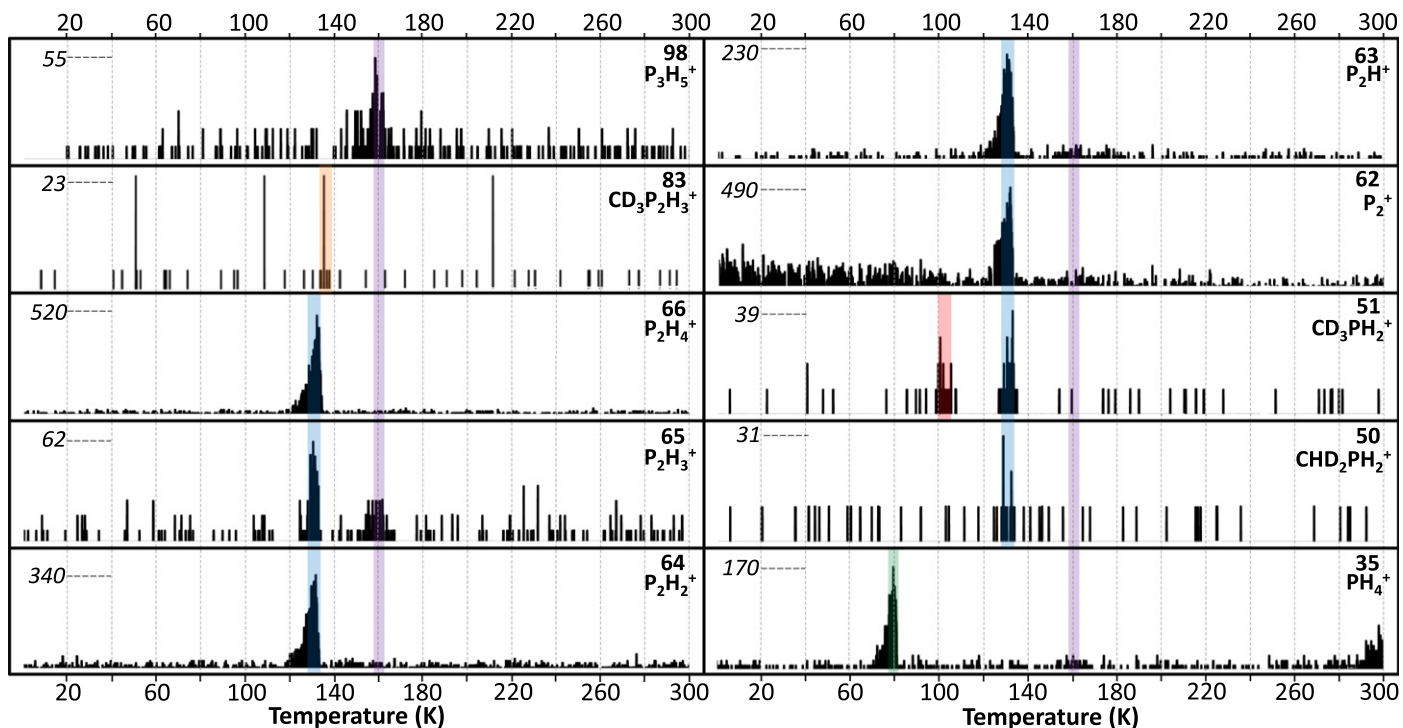


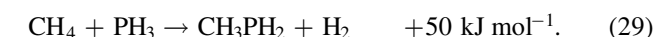
**Figure 12.** Quadrupole mass spectra for the products of phosphine ( $\text{PH}_3$ ) and deuterated methane ( $\text{CD}_4$ ). The intensity (in thousands) is listed on the left while the mass-to-charge and ionic formula are on the right.

### 4.3. Energetics

Using experimental reaction energies (Chase 1998), we now consider the energy necessary to form the observed products. The preferred pathway (reaction (6)) toward formation of methylphosphine ( $\text{CH}_3\text{PH}_2$ ) requires the recombination of the

phosphino ( $\text{PH}_2$ ) and methyl ( $\text{CH}_3$ ) radicals. To remove one hydrogen from their parent compounds,  $339 \text{ kJ mol}^{-1}$  (3.51 eV) and  $439 \text{ kJ mol}^{-1}$  (4.55 eV) are needed, respectively (reactions (25a) and (26a)). This energy necessary for bond cleavage is supplied by the energetic electrons. The barrierless

methyl and phosphino radical recombination (reaction (27)) releases  $291 \text{ kJ mol}^{-1}$  (3.01 eV), and thus the reaction energy for bond cleavage followed by methyl and phosphino radical recombination (reaction (28)) is  $+486 \text{ kJ mol}^{-1}$  (5.04 eV). The overall reaction including molecular hydrogen formation (reaction (29)) is endoergic by  $50 \text{ kJ mol}^{-1}$  (0.52 eV). Compared to removing the first hydrogen, only slightly more energy is necessary to remove a second hydrogen from phosphine or methane and form phosphinidene and carbene (reactions (25b) and (26b)). However, an additional  $90 \text{ kJ mol}^{-1}$  (0.94 eV) and  $38 \text{ kJ mol}^{-1}$  (0.39 eV), respectively, is necessary to promote these radicals to their first excited singlet state (reactions (25c) and (26c)), which allows them to insert barrierlessly. With minimal thermal energy available at 5.5 K, the reaction must involve non-equilibrium chemistry to proceed. Non-irradiated blank experiments showed that no reactions occurred, confirming that thermal chemistry cannot create these products at such low temperatures. Each of the three mechanisms shown to produce methylphosphine—radical recombination, phosphinidene insertion, and carbene insertion—is capable of barrierless methylphosphine formation. The endoergic nature of the reaction indicates that non-equilibrium chemistry initiated by high energy particles such as galactic cosmic rays are necessary in interstellar conditions, but once this initial energy is supplied the reaction proceeds favorably and barrierlessly. Furthermore, these reaction intermediates can spontaneously produce the products seen in this study if they are present in the first monolayer and within close proximity without the need for ionizing radiation nor diffusion through the ice:



## 5. CONCLUSION

Ices of phosphine with methane and deuterated methane that were irradiated with energetic electrons at 5.5 K produced a homologous series of phosphanes from  $\text{P}_2\text{H}_4$  to  $\text{P}_8\text{H}_{10}$  and methylphosphanes from  $\text{CH}_3\text{PH}_2$  to  $\text{CH}_3\text{P}_8\text{H}_9$ . All observed products were phosphorus-containing but the products that also contain carbon have exactly one carbon atom. Because the group frequencies of the products from phosphine and methane irradiation overlap significantly with the parent peaks, FTIR had limited use in this type of study and diphosphine was the only product that could be quantified. Furthermore, quadrupole mass spectrometry with electron impact ionization observed only diphosphine, methylphosphine, methylidiphosphine, and triphosphane. On the other hand, ReTOF mass spectrometry could observe molecular ions as large as  $\text{P}_3\text{H}_7^+$  and  $\text{CH}_3\text{P}_4\text{H}_5^+$ , while  $\text{P}_8\text{H}_{10}$  and  $\text{CH}_3\text{P}_8\text{H}_9$  could be identified from their fragments from  $\text{PH}_2$  loss, which is the most common fragmentation pathway. Using deuterated methane results as evidence, a signal at  $m/z = 81$  confirms the formation of

methylenediphosphine ( $\text{PH}_2\text{CHDPH}_2$ ) and, in addition to  $m/z = 51$  ( $\text{CHD}_2\text{PH}_2$ ), the formation of methylphosphine via carbene insertion. The signals at  $m/z = 52$  ( $\text{CD}_3\text{PHD}$ ) and  $m/z = 84$  ( $\text{CD}_4\text{H}_2\text{P}_2$ ) also confirm the formation of methylphosphine via phosphinidene insertion. However, radical recombination, which contributed to the intense signals at  $m/z = 51$  ( $\text{CD}_3\text{PH}_2$ ) and  $m/z = 83$  ( $\text{CD}_3\text{P}_2\text{H}_3$ ), was the most likely formation pathway. The overall reaction forming methylphosphine ( $\text{CH}_3\text{PH}_2$ ) is endoergic by  $+50 \text{ kJ mol}^{-1}$  (0.52 eV), which makes this compound unlikely in cold environments that rely solely on thermal chemistry. However, our results show that energetic particles like galactic cosmic rays can induce non-equilibrium chemistry that not only forms methylphosphine but a suite of higher order phosphanes and methylphosphanes, and thus methylphosphine can be expected in cold interstellar environments with sufficient quantities of phosphine and methane. Methylphosphine contains a carbon-phosphorus single bond, which has yet to be observed in the interstellar medium but has been discovered in the C1 to C4 alkylphosphonic acids contained in the Murchison meteorite (Cooper & Cronin 1992), which verifies that the carbon-phosphorus single bond can be produced in extra-terrestrial environments, although their ultimate origins remain elusive. These results also have potential implications to the chemistry of planetary atmospheres, as phosphine (Ridgway & Smith 1976; Larson et al. 1980) and methane (Ehrenfreund & Charnley 2000) have been discovered on Jupiter and Saturn. Future work can look into the abundance of individual isomers, such as methylenediphosphine ( $\text{PH}_2\text{CH}_2\text{PH}_2$ ) and methylidiphosphine ( $\text{CH}_3\text{P}_2\text{H}_3$ ), by performing selective VUV photo-ionization experiments utilizing four-wave difference and sum mixing (Hilbig & Wallenstein 1982; VonDrasek et al. 1988) to further investigate the most likely reaction pathways. Also, more complex mixtures, such as the addition of water or carbon monoxide, can be explored to synthesize potential interstellar compounds in more astrophysically relevant ices.

The authors would like to thank the WM Keck Foundation (RIK) and the University of Hawaii (AMT, MJA) for support.

## APPENDIX

The use of an RGA (QMS) is common with experiments that detect products that sublime into the gas phase, and we utilize one in tandem with the ReTOF to compare the sensitivity of these techniques. It should be stressed that molecular sublimation and sputtering from the ice is negligible during the irradiation phase, and previous findings demonstrate that low currents of high energy electrons are inefficient at causing sputtering in low temperature ices at typically 5–10 K (Bahr et al. 2001; Baragiola et al. 2003). During the TPD phase, diphosphine ( $\text{P}_2\text{H}_4$ ) contributed the most interesting results in the RGA mass spectra for phosphine and methane ( $\text{CH}_4$ ) irradiated ice (Figure 11 and Table 5). Unlike the ReTOF,  $\text{P}_2\text{H}_4$  fragmented even down to  $\text{P}_2^+$  via dissociative electron impact ionization. The other products seen,  $\text{P}_3\text{H}_5$ ,  $\text{CH}_3\text{PH}_2$ , and  $\text{CH}_3\text{P}_2\text{H}_3$ , occurred at low intensities. The results for phosphine with deuterated methane ( $\text{CD}_4$ ) (Figure 12 and Table 6) were identical for  $\text{P}_2\text{H}_4$  and  $\text{P}_3\text{H}_5$ , and two isotopologues of  $\text{CH}_3\text{PH}_2$  appeared: a strong  $m/z = 51$  ( $\text{CD}_3\text{PH}_2$ ) signal and an  $m/z = 50$  ( $\text{CHD}_2\text{PH}_2$ ) signal that barely appeared above background levels. Similar to the ReTOF results,  $\text{CD}_3\text{PH}_2$

was the most abundant form of methylphosphine, although the RGA intensities are too small for a quantitative comparison. Only tenuous amounts of  $\text{CD}_3\text{P}_2\text{H}_3$  were seen at  $m/z = 83$ . Thus, the ReTOF was a far more sensitive mass spectrometry method, as it was capable of detecting 15 products for the phosphine and methane ice mixture compared to only four products using the RGA, and three isotopologues of methylphosphine were seen and quantitatively compared using the ReTOF, while the RGA detected only two isotopologues.

## REFERENCES

- Agundez, M., Cernicharo, J., Decin, L., Encrenaz, P., & Teyssier, D. 2014a, *ApJL*, **790**, L27
- Agúndez, M., Cernicharo, J., & Guélin, M. 2007, *ApJL*, **662**, L91
- Agundez, M., Cernicharo, J., & Guélin, M. 2014b, *A&A*, **570**, A45
- Agundez, M. C. J., Pardo, J., Guélin, M., & Phillips, T. 2008, *A&A*, **485**, L33
- Babar, S., & Weaver, J. 2015, *ApOpt*, **54**, 477
- Bahr, D., Fama, M., Vidal, R., & Baragiola, R. 2001, *JGRE*, **106**, 33285
- Baragiola, R., Vidal, R., Svendsen, W., et al. 2003, *NIMPB*, **209**, 294
- Bennett, C. J., Brotton, S. J., Jones, B. M., et al. 2013, *AnaCh*, **85**, 5659
- Bennett, C. J., Jamieson, C. S., Osamura, Y., & Kaiser, R. I. 2006, *ApJ*, **653**, 792
- Bennett, C. J., & Kaiser, R. I. 2007, *ApJ*, **660**, 1289
- Brunetto, R., Caniglia, G., Baratta, G. A., & Palumbo, M. E. 2008, *ApJ*, **686**, 1480
- Chase, M. W. 1998, NIST-JANAF Thermochemical Tables, 4th edn, JPCRD, Monograph No. 9 (New York: AIP)
- Cooper, G. O. W., & Cronin, J. 1992, *GeCoA*, **56**, 4109
- Cottrell, T. L. 1954, *The Strengths of Chemical Bonds* (New York: Academic)
- Durig, J., Shen, Z., & Zhao, W. 1996, *JMoSt*, **375**, 95
- Ehrenfreund, P., & Charnley, S. B. 2000, *ARA&A*, **38**, 427
- Fourikis, N., Takagi, K., & Morimoto, M. 1974, *ApJL*, **191**, L139
- Francia, M. D., & Nixon, E. R. 1973, *JCP*, **58**, 1061
- Fueno, T., Bonacic-Koutecky, V., & Koutecky, J. 1983, *JACS*, **105**, 5547
- Fulvio, D., Sivaraman, B., Baratta, G., et al. 2009, *AcSpA*, **72**, 1007
- Goodman, A. M. 1978, *ApOpt*, **17**, 2779
- Gordon, M. S., Boatz, J., Gano, D. R., & Friedrichs, M. G. 1987, *JACS*, **109**, 1323
- Guélin, M., Cernicharo, J., Paubert, G., & Turner, B. 1990, *A&A*, **230**, L9
- Guélin, M., Muller, S., Cernicharo, J., et al. 2000, *A&A*, **363**, L9
- Halfen, D., Clouthier, D., & Ziurys, L. M. 2008, *ApJL*, **677**, L101
- Halfen, D. T., Clouthier, D. J., & Ziurys, L. M. 2014, *ApJ*, **796**, 36
- Hilbig, R., & Wallenstein, R. 1982, *ApOpt*, **21**, 913
- Hodges, R. V., McDonnell, T., & Beauchamp, J. 1980, *JACS*, **102**, 1327
- Holtom, P., Osamura, B. C., Mason, N., & Kaiser, R. 2005, *ApJ*, **626**, 940
- Hovington, P., Drouin, D., & Gauvin, R. 1997, *Scanning*, **19**, 1
- Hudgins, D., Sandford, S., Allamandola, L., & Tielens, A. 1993, *ApJSS*, **86**, 713
- Johnson, R. D., III., 2015, NIST Computational Chemistry Comparison and Benchmark Database, NIST Standard Reference Database Number 101, Release 17b <http://cccbdb.nist.gov/>
- Jones, B. M., & Kaiser, R. I. 2013, *J. Phys. Chem. Lett.*, **4**, 1965
- Jones, B. M., Kaiser, R. I., & Strazzulla, G. 2014a, *ApJ*, **781**, 85
- Jones, B. M., Kaiser, R. I., & Strazzulla, G. 2014b, *ApJ*, **788**, 170
- Kaifu, N., Morimoto, M., Nagane, K., et al. 1974, *ApJL*, **191**, L135
- Kaiser, R., Eich, G., Gabrysch, A., & Roessler, K. 1997, *ApJ*, **484**, 487
- Kaiser, R. I., Maity, S., & Jones, B. M. 2014, *PCCP*, **16**, 3399
- Kaiser, R. I., Maity, S., & Jones, B. M. 2015, *Angew Chem Int Edit*, **54**, 195
- Kim, H.-W., Chechla, A. A., & Kim, B. 2007, *JMoSt*, **802**, 105
- Kim, Y. S., & Kaiser, R. I. 2011, *ApJ*, **729**, 68
- Lafont, S., Lucas, R., & Omont, A. 1982, *A&A*, **106**, 201
- Larson, H., Fink, U., Smith, H., & Davis, D. 1980, *ApJ*, **240**, 327
- Li, H. H. 1976, *JPCRD*, **5**, 329
- Maity, S., Kaiser, R., & Jones, B. M. 2014a, *ApJ*, **789**, 36
- Maity, S., Kaiser, R. I., & Jones, B. M. 2014b, *FaDi*, **168**, 485
- Maity, S., Kaiser, R. I., & Jones, B. M. 2015, *PCCP*, **17**, 3081
- Maksyutenko, P., Muzangwa, L. G., Jones, B. M., & Kaiser, R. I. 2015, *PCCP*, **17**, 7514
- Milam, S., Halfen, D., Tenenbaum, E., et al. 2008, *ApJ*, **684**, 618
- Milam, S. N. 2007, Doctoral thesis, Univ. Arizona
- Ridgway, S. W. L., & Smith, G. 1976, *ApJ*, **207**, 1002
- Satorre, M., Domingo, M., Millán, C., et al. 2008, *P&SS*, **56**, 1748
- Staley, R. H., & Beauchamp, J. L. 1974, *JACS*, **96**, 6252
- Tenenbaum, E., Woolf, N., & Ziurys, L. 2007, *ApJL*, **666**, L29
- Tenenbaum, E., & Ziurys, L. 2008, *ApJL*, **680**, L121
- Turner, A. M., Abplanalp, M. J., Chen, S., et al. 2015, *PCCP*, **17**, 27227
- Turner, B., & Bally, J. 1987, *ApJL*, **321**, L75
- VonDrasek, W. A., Okajima, S., & Hessler, J. P. 1988, *ApOpt*, **27**, 4057
- Westley, M., Baratta, G., & Baragiola, R. 1998, *JCP*, **108**, 3321
- Ziurys, L. 1987, *ApJL*, **321**, L81